

LA-UR-24-24036

Accepted Manuscript

A cell-based Papain-like Protease (PLpro) activity assay for rapid detection of active SARS-CoV-2 infections and antivirals

Velappan, Nileena; Jumenz, Anahi; Maestas, Lucas I; Beck, Brian; Ye, Chunyan Ye; Wensing, Keith; Mata-Solis, Yaniksa; Bruno, William; Bussman, Silas; Bradfute, Steven B.; Baca, Justin; Rininsland, Frauke

Provided by the author(s) and the Los Alamos National Laboratory (1930-01-01).

To be published in: PLOS ONE

DOI to publisher's version: 10.1371/journal.pone.0309305

Permalink to record:

<https://permalink.lanl.gov/object/view?what=info:lanl-repo/lareport/LA-UR-24-24036>



Los Alamos National Laboratory, an affirmative action/equal opportunity employer, is operated by Triad National Security, LLC for the National Nuclear Security Administration of U.S. Department of Energy under contract 89233218CNA000001. By approving this article, the publisher recognizes that the U.S. Government retains nonexclusive, royalty-free license to publish or reproduce the published form of this contribution, or to allow others to do so, for U.S. Government purposes. Los Alamos National Laboratory requests that the publisher identify this article as work performed under the auspices of the U.S. Department of Energy. Los Alamos National Laboratory strongly supports academic freedom and a researcher's right to publish; as an institution, however, the Laboratory does not endorse the viewpoint of a publication or guarantee its technical correctness.

RESEARCH ARTICLE

A cell-based Papain-like Protease (PLpro) activity assay for rapid detection of active SARS-CoV-2 infections and antivirals

Anahi G. Jimenez-Campos¹✉, Lucas I. Maestas¹✉, Nileena Velappan², Brian Beck³, Chunyan Ye⁴, Keith Wernsing⁵, Yaniksa Mata-Solis⁵, William J. Bruno⁶, Silas C. Bussmann¹✉, Steven Bradfute⁴, Justin T. Baca¹✉, Frauke H. Rininsland^{5*}

1 University of New Mexico Health Sciences Center, Department of Emergency Medicine, Albuquerque, New Mexico, United States of America, **2** Los Alamos National Laboratory, Los Alamos, NM, United States of America, **3** MicroBiologics, St. Cloud, MN, United States of America, **4** Health Science Center, Center for Global Health and Department of Internal Medicine, University of New Mexico, Albuquerque, New Mexico, United States of America, **5** Mesa Photonics, Santa Fe, NM, United States of America, **6** SciTransTech, Santa Fe, NM, United States of America

✉ These authors contributed equally to this work.

* frininsland@mesaphotonics.com



OPEN ACCESS

Citation: Jimenez-Campos AG, Maestas LI, Velappan N, Beck B, Ye C, Wernsing K, et al. (2024) A cell-based Papain-like Protease (PLpro) activity assay for rapid detection of active SARS-CoV-2 infections and antivirals. PLoS ONE 19(12): e0309305. <https://doi.org/10.1371/journal.pone.0309305>

Editor: Mirko Cortese, Telethon Institute of Genetics and Medicine, ITALY

Received: June 10, 2024

Accepted: August 9, 2024

Published: December 26, 2024

Copyright: © 2024 Jimenez-Campos et al. This is an open access article distributed under the terms of the [Creative Commons Attribution License](https://creativecommons.org/licenses/by/4.0/), which permits unrestricted use, distribution, and reproduction in any medium, provided the original author and source are credited.

Data Availability Statement: All data are in the manuscript and/or [supplemental information](#) files.

Funding: The research was funded by the Department of Defense, Defense Logistics Agency (SP4701-21-C-0054) to Mesa Photonics. Technical assistance for cell-based assays using non-SARS-CoV-2 coronaviruses was provided by Los Alamos National Laboratory through the New Mexico Small Business Assistance (NMSBA) program. The funders had no role in the study design, data

Abstract

Severe acute respiratory syndrome coronavirus 2 (SARS-CoV-2) and its variants are a continuous threat to human life. An urgent need remains for simple and fast tests that reliably detect active infections with SARS-CoV-2 and its variants in the early stage of infection. Here we introduce a simple and rapid activity-based diagnostic (ABDx) test that identifies SARS-CoV-2 infections by measuring the activity of a viral enzyme, Papain-Like protease (PLpro). The test system consists of a peptide that fluoresces when cleaved by SARS PLpro that is active in crude, unprocessed lysates from human tongue scrapes and saliva. Test results are obtained in 30 minutes or less using widely available fluorescence plate readers, or a battery-operated portable instrument for on-site testing. Proof-of-concept was obtained in a study on clinical specimens collected from patients with COVID-19 like symptoms who tested positive ($n = 10$) or negative ($n = 10$) with LIAT RT-PCR using nasal mid turbinate swabs. When saliva from these patients was tested with in-house endpoint RT-PCR, 17 were positive and only 5 specimens were negative, of which 2 became positive when tested 5 days later. PLpro activity correlated in 17 of these cases (3 out of 3 negatives and 14 out of 16 positives, with one invalid specimen). Despite the small number of samples, the agreement was significant (p value = 0.01). Two false negatives were detected, one from a sample with a late Ct value of 35 in diagnostic RT-PCR, indicating that an active infection was no longer present. The PLpro assay is easily scalable and expected to detect all viable SARS-CoV-2 variants, making it attractive as a screening and surveillance tool. Additionally, we show feasibility of the platform as a new homogeneous phenotypic assay for rapid screening of SARS-CoV-2 antiviral drugs and neutralizing antibodies.

collection and analysis, decision to publish or preparation of the manuscript.

Competing interests: Mesa Photonics holds two utility patents covering diagnostics of SARS-CoV-2 infections and antiviral screening based on PLpro activity: US11603552B2, Method for pathogen identification, Inventors: Frauke Henrike Rininsland, Daniel James Kane, Application granted: 2023-03-14 and US11851698B2, Method for pathogen identification, Continuation of US11603552B2, Inventors: Frauke Henrike Rininsland, Daniel James Kane, Application granted: 2023-12-26. The other authors declare no conflict of interest. This does not alter our adherence to PLOS ONE policies on sharing data and materials.

Introduction

Since the emergence of the severe acute respiratory syndrome coronavirus 2 (SARS-CoV-2) in 2019, over 2,200 different diagnostic tests have been developed and introduced to the market targeting either SARS-CoV-2 nucleic acids or antigens [1]. In addition, promising novel tests have been developed including electrochemical sensing of the SARS-CoV-2 spike protein or RNA, colorimetric naked eye detection of SARS-CoV-2 RNA, or detection of volatile organic compounds in breath common to infection with different variants of the SARS-CoV-2 [2–6].

The SARS-CoV-2 Papain-Like protease (PLpro) and the main protease (MPro, also known as 3CLPro) present a third class of detection targets that have been used to detect SARS-CoV-2 infections [7–9]. PLpro and MPro cleave the viral polyprotein at conserved sites to separate the non-structural proteins nsp 1–3 and nsp 4–16, respectively [10, 11]. Release of the nsp proteins is essential for viral replication as 15 nsps compose the viral replication and transcription complex (RTC) [12]. In addition to cleaving the viral polyprotein, SARS-CoV-2 PLpro cleaves the LXGG amino acid sequence in ubiquitin and interferon induced gene 15 (ISG15) with a strong substrate preference for ISG15 compared to ubiquitin, thus counteracting the host innate immune response that is initiated when ISG15 is conjugated to cellular proteins [9, 13, 14]. The dual function of SARS-CoV-2 PLpro makes it an attractive target for antiviral drugs that could inhibit not only viral propagation but restore the host innate immune response as well [15].

Novel methods for measuring SARS-CoV-2 PLpro activities in infected cells include dually labeled fluorescent probes or a cleavable peptide-DNA nanoprobe based electrochemical sensor [8, 16]. However, the activity of PLpro appears to be affected by the chemical structure of the fluorescent probe, leading to 3-hour long incubation times for detection, while the electrochemical sensing approach is complicated by several processing steps, thus limiting the usefulness of these approaches for point of care testing (POCT).

We report here on rapid (<30 minutes), homogeneous POC test that measures the proteolytic activity of SARS-CoV-2 PLpro using synthetic peptides that are recognized by SARS-CoV-2 PLpro and fluoresce when cleaved. This kind of assay belongs to a category known as activity-based diagnostics (ABDx) that are gaining recognition as important methodologies for detecting pathogen infections in clinical specimens or cancer [7, 17–21].

The approach has several advantages.

PLpro activity assays detect only active infections

SARS-CoV-2 proteases are expressed only in infected cells that are actively assembling new virions; therefore, measuring viral protease activity is likely to accurately identify only those individuals able to transmit infectious virus. In contrast, RT-PCR cannot differentiate between replication competent virus and residual, non-infectious RNA that in some cases has been detected 28 days or even months after symptoms have cleared [22, 23]. Currently, the presence of infectious virus is assessed in cell culture by determining the cytopathic effect (CPE), detecting viral fragments by RT-PCR or immunostaining, using plaque assays, focus-forming assays, or by determining the 50% tissue culture infectious dose (TCID₅₀) [24, 25]. These methods cannot be used for routine specimen testing since they are time- and labor intensive and restricted to biosafety level 3 conditions. Negative sense SARS-CoV-2 RNA, which is produced only by replicating virus, can also be used as an indicator of infectiousness, but this type of testing is not inexpensive or rapid, and therefore not suitable for population screening [26]. Due to these limitations, at the beginning of the pandemic a patient's ability to transmit virus was predicted by the arbitrary test-specific cycle threshold (Ct) value determined in RT-PCR, but this approach has since proved unreliable [27–30].

Protease activities are detectable early in an infection

After SARS-CoV-2 has entered a cell, intracellular virions are produced within 10 hours but typically not released from the cell until 72 hours postinfection [31, 32]. Since the SARS-CoV-2 proteases PLpro and MPro are required for the production of intracellular virions, it is expected that their activities are detectable in infected cells several days before RNA is collectable from extracellular virions that are shed into specimens. As a result, RT-PCR tests typically perform best 2 days after symptom onset when viral loads are highest, missing pre-symptomatic and asymptomatic transmission [33]. One study suggests a sensitivity approaching 0% corresponding to a false negative rate of nearly 100% at the early stages of infection, including periods when at least some people are already infectious [34]. Early detection of infection by measuring protease activities would facilitate the rapid isolation of infected people and early treatment of the vulnerable population.

Detection of protease activities is likely “variant proof”

SARS-CoV-2 proteases do not tolerate mutations in the catalytic domains that would interfere with their cleavage activities and thereby cause a false negative test result with an ABDx test. A recent analysis of 70,000 PLpro sequences identified mutations in only 5%, all in regions outside of the catalytically active domains [35]. It is therefore highly likely that PLpro activity is measurable in any of the continuously emerging SARS-CoV-2 variants that may be missed by RT-PCR when primers or probes fail to bind to mutated sequences. One study reported that 4–5 individual variants may coexist in one person in which 79% of primer binding sequences in at least 1 genome were mutated, with the result that 10–15% of variants were not detectable [36–38].

Cell-based protease activity assays for screening of SARS-CoV-2 antivirals

Although both SARS-CoV-2 MPro and PLpro are attractive drug targets, so far only one targeted therapy—the MPro inhibitor nirmatrelvir (a component of Paxlovid)—has received approval for use in the United States [39, 40]. Despite the considerable efforts that have been invested in the development of PLpro inhibitors, promising lead candidates have not progressed to animal models. One possible reason is that many studies have used recombinant enzyme containing only the minimal proteolytic PLpro domain to screen for compound inhibition in biochemical screens, neglecting the effects of other SARS-CoV-2 domains involved in regulating the activity of natural PLpro in cells [41]. Although these limitations can be overcome using phenotypic assays, these tests require several steps and 5–7 days to measure the effect of drugs on cell proliferation or health. Promising new drug candidate have been identified using a cell-based FlipGFP-based reporter assay; however, this recombinant reporter PLpro also does not reflect the natural PLpro as it is produced by the cell [42].

Further, measuring SARS-CoV-2 protease activity as a marker of infection allows to rapidly determine the efficacy of therapeutic or vaccine-derived antibodies. Neutralization assays, such as plaque reduction neutralization test (PRNT), fluorescent antibody virus neutralization (FAVN) assays and immunological assays, play a pivotal role in evaluating the efficacy of vaccines, selecting convalescent plasma for clinical trials and therapeutic use, and defining immune evasion [43]. However, those assays require several steps and days to complete [43]. In contrast, cell-based protease activity assays are simple and can be automated and completed in one working day with minimal user steps.

We report here on an ABDx platform optimized for detecting the activity of SARS-CoV-2 Papain-like protease (PLpro) in crude, active lysates from infected cells. We show proof of concept as a Point of Care (PoC) diagnostic test by demonstrating the ability to detect SARS-CoV-

2 PLpro activity in unprocessed lysates from patient saliva or tongue scrape specimens in a clinical feasibility study. A second study showed high percent agreement with endpoint RT-PCR in saliva specimens. Additional data highlight the potential of the platform as a faster and safer alternative to current phenotypic assays that could accelerate the discovery of antiviral drugs and neutralizing antibodies.

Materials and methods

Assay principle

We used fluorescence “turn on” assays for SARS-CoV-2 PLpro and Mpro in which lysates are incubated with a peptide labeled with a fluorophore at the terminal amino acid. In the intact peptide, the fluorescence is quenched by the electrons in the amide bonds and restored when the protease cleaves the bond between the terminal amino acid of the peptide and the fluorophore (Fig 1).

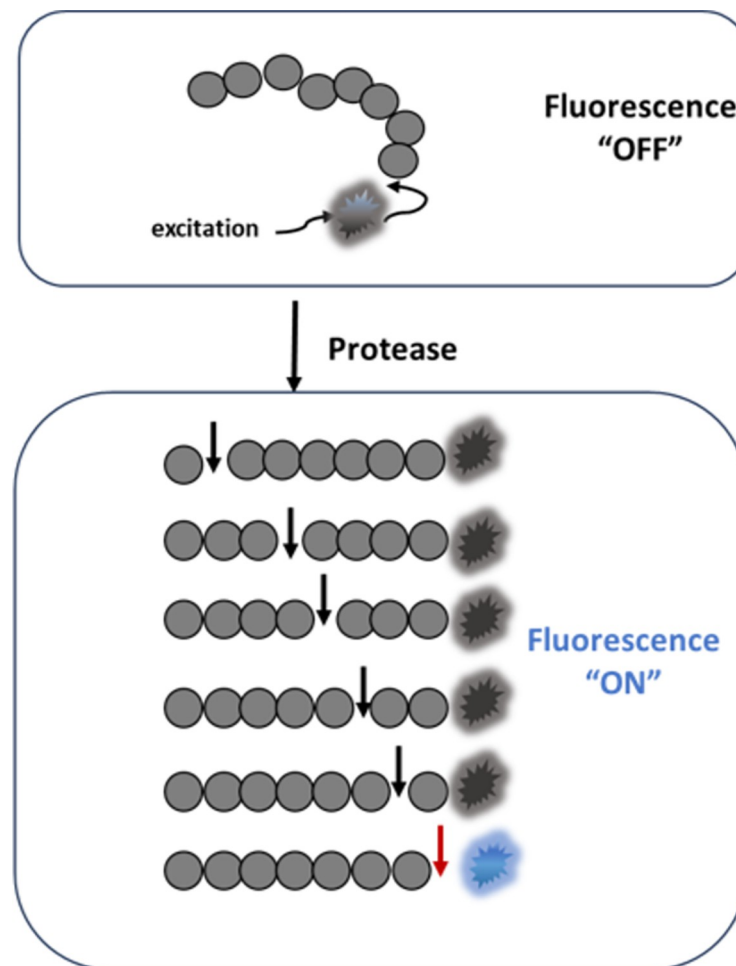


Fig 1. Schematic of the SARS-CoV-2 protease fluorescence turn on assay. The assay uses peptides composed of amino acids (grey circles) that are cleaved by the protease of interest and a fluorophore (starburst) conjugated to the terminal amino acid. In the intact peptide, the fluorescence is quenched by the electron withdrawing property of the amide bond. Fluorescence is restored (blue starburst) only when cleavage occurs at the bond between the terminal amino acid and the fluorophore (red arrow). Cleavage between amino acids (black arrows) by other proteases that may be present in a crude lysate does not result in notable fluorescence (grey starburst). Peptides used in this study were labeled at the carboxy terminus with rhodamine 110 (R110) or amino 7-amino-4-methylcoumarin (AMC).

<https://doi.org/10.1371/journal.pone.0309305.g001>

Biochemical enzyme activity assays

Peptides. PLpro peptide substrates consisted of various stretches of amino acids from human or mouse ISG15, which PLpro is known to preferably bind and cleave, conjugated to the known terminal PLpro cleavage sequence LRGG (see Table 1) [44].

Peptides P4-AMC and P16-AMC were 4 and 16 amino acids in length and labeled with 7-amino-4-methylcoumarin (AMC). P4-AMC was purchased from BioTechnie, (Minneapolis, MN) and P16-AMC synthesized by LifeTein (Somerset, NJ). PLpro peptides containing unnatural amino acids in the cleavage sequence (denoted as “Pun”) were used in cell-based assays. The peptides Pun16 and Pun74 were 16 and 74 amino acids in length and synthesized and labeled with AMC or rhodamine 110 (R110) at the carboxy terminus by LifeTein and AmbioPharm (Beech Island, SC). ISG15-R110 was purchased from SouthBay BioScience (San Francisco, CA) or from UBPBio (Amsterdam, The Netherlands), ISG15-AMC was from R&D Systems and ubiquitin-AMC from UBPBio.

The MPro peptide with the sequence LGS AVLQ-rhodamine110-dP was purchased from R&D Systems (Minneapolis, MN). This peptide is cleaved after glutamine (Q) by MPro from coronaviruses but rarely by other human proteases [9].

Internal control peptides were used to demonstrate that lysates were of sufficient quality and quantity for the assay to perform. The peptide with the sequence FITC-YVADAP-DNP (Bachem, Vista, CA) is cleaved by the Angiotensin Converting Enzyme 2 (ACE2) and the peptide with the sequence DEVD by caspases. DEVD peptides were labeled with AMC or R110 and purchased from R&D Systems (Minneapolis, MN).

Enzymes. Recombinant papain-like proteases (PLPs) from SARS-1, SARS-CoV-2, NL63 and caspase 3 were purchased from BPS BioScience (San Diego, CA). Recombinant USP18 was obtained from Boston Biochemicals and AdenoL3 protease from MyBiosource (San Diego, CA, #MBS1182235_61). Recombinant PLPs from MERS, OC43, 229E and HKU1 were produced by Genscript (Piscataway, NJ) and contained amino acids spanning the active site and UBL-1 sites. MERS (Genbank accession number AFS88944) contained amino acids 1482–1802, OC43 (Genbank accession number AMK59674) amino acids 1562–1870, 229E (Genbank accession number APT69896) amino acids 1590–1904, and HKU1 (Genbank accession number ARB07606) amino acids 1642–1957. Genes were synthesized and codon optimized, cloned into the EcoRI/HindIII cloning sites of the pcDNA3.4 vector, transfected into Chinese Hamster Ovary cells (CHO-S), and purified via HIS tag according to protocols established at

Table 1. IDs, targets, and sequences of peptides used in this study.

Peptide ID	Target	Sequence
P4-AMC	PLPro	Z-LRGG-AMC
P16-AMC	PLPro	Ac-LKPLSTVFMNLR LRGG-AMC
Pun16-AMC	PLPro	Ac-LKPLSTVFMNLR-{hTyr}-{Dap}-GG-AMC
Pun16-R110	PLPro	Ac-LKPLSTVFMNLR-{hTyr}-{Dap}-GG-R110
Pun74-R110	PLPro	Ac-SEPLSILVRNERGHSNIYEVFLTQTVDTLKKKVSQREQVHEDQFWLSFEGRPMEDKELL GEYGLKPQSTVIKHLR-{hTyr}-{Dap}-GG-R110
ISG15-R110	PLPro	Full-length, mature ISG15 polypeptide, amino acids 2–157 (see South Bay Bio, Cat. #SBB-PS0002)
ISG15-AMC	PLPro	Recombinant full length (see RnD Systems Cat. #UL553)
Ubiquitin-AMC	PLPro	MQIFVKTLTGKTTITLEVEPSDTIENVKAKIQDKEGIPPDQQLRFIFAGKQLEDGRTLSDYNIQKESTLHLVLR LRGG-AMC (see UBPBio, Cat. # M3010)
	MPro	LGS AVLQ-R110-dP
	ACE2	FITC-YVADAP-DNP
	Caspase	(DEVD) ₂ -R110

<https://doi.org/10.1371/journal.pone.0309305.t001>

Genscript. The quality of the proteins was confirmed by SDS-PAGE, Western blot and analytical SEC-HPLC.

Papain-like proteases. Biochemical assays using recombinant proteases were performed to optimize SARS-CoV-2 PLpro assay conditions, characterize, and optimize PLpro substrates, and to test for cross reactive cleavage by other papain-like proteases. Assays were performed in 20 μ l assay buffer (50mM HEPES, 5mM DTT, 1x lysis buffer, pH 7.4) using substrate concentrations ranging from 2 μ M to 20 μ M. The final concentrations of recombinant PLPs from SARS-CoV and SARS-CoV-2 were 100nM, NL63 428nM, MERS 1178nM, OC43 1760nM, 229E 1200nM and HKU1 1200nM. The fluorescence from cleaved AMC or R110 was measured using excitation and emission wavelengths of $\lambda_{\text{ex}} = 365\text{nm}$ and $\lambda_{\text{em}} = 465\text{nm}$ for AMC and $\lambda_{\text{ex}} = 485\text{nm}$ and $\lambda_{\text{em}} = 528\text{nm}$ for R110-labeled substrates in a fluorescence plate reader (Synergy H1, Agilent Technologies, Santa Clara, California) in white 384-well plates (Corning Inc., Corning, NY).

MPro. MPro assays were performed using the same assay buffer as for PLpro, with 10 μ M peptide and between 5nM and 500nM enzyme.

Caspase-3. Internal control assays were performed using the assay buffer as above, 1.5nM caspase 3, and 10 μ M peptide (DEVD₂-R110). In some assays, PLpro and caspase peptides labeled with different fluorophores were combined and monitored in one reaction using dual wavelength monitoring for AMC and R110.

USP18. USP18 (1000nM) was reacted with human ISG15-R110 (500nM) in assay buffer containing 50 mM HEPES, pH 7.5, 10 mM DTT, 0.01% Tween.

Adenovirus protease L3. Enzyme (250nM) was reacted with 66 μ M peptide P4 or Pun4 in 25mM TRIS-HCL, pH 7.4, 2mM DTT, 0.3% octylglucoside.

Sample quantification (“Quanti Dye”). The nucleic acid content in lysates was measured to estimate the amount of biological material collected in tongue scrape and saliva specimens. The nucleic acid intercalating dye SYBR[®] Safe Stain (Edvotek, Washington, DC) was used at a 2.5x dilution in 100mM HEPES, pH 7.4. The linear region of detection was determined by adding QuantiDye to triplicate wells of crude lysate that was diluted in steps of 1:2 in lysis buffer. The linear detection range was between 74,000 RFU to > 1.5 million RFU (S1 Fig).

HCoV NL63, OC43, 229E infection and cell-based activity assays

All experiments with HCoV propagation were performed in biosafety level 2 containment laboratories at Los Alamos National Laboratory with approved protocols. MRC-5 cells (ATCC, CCL-171), HCT8 cells (ATCC, CCL-244), and LLC-MK2 cells (ATCC, CCL-7) were grown to 90% confluency (approx. 1×10^5 cells per well) in 12-well plates in Dulbecco's minimal essential medium (DMEM) supplemented with 10% fetal calf serum (FCS) and 1% penicillin/streptomycin. MRC-5 cells were infected with 2 multiplicities of infection (MOI) of 229E (ATCC, VR-740) for 24 hours, HCT-8 with 2 MOI of OC43 (ATCC, VR-1558) for 5 days, and LLC-MK2 with 1 MOI of NL63 (BEI NR-470) for 24 hours in viral growth medium (MEM + 2.5% heat inactivated fetal calf serum) at 37°C in a humidified incubator.

HCoV OC43, 229E and NL63 protease activity assays. After cells were incubated with virus, the media was removed from the wells and cells washed three times with 100mM HEPES. Lysis buffer (500 μ l, Mesa Photonics) was added to each well, incubated for 5 minutes at room temperature and 40 μ l of lysates added to duplicate wells of a 96 well white plate (Greiner). Peptides (40 μ l) in 2x assay buffer (100mM HEPES, 10mM DTT, pH 7.4) were added to the wells to achieve final concentrations of 2.5 μ M ACE2 peptide (FITC-YVADAPK-DNP) and 100nM of Ubiquitin-AMC and 100nM ISG15-AMC. Fluorescence was read after 15 minutes and 1 hour in a fluorescence plate reader (Tecan Infinite, Morgan Hill, CA) with a 3

second shake between reads using $\lambda_{\text{ex}} = 365\text{nm}$ and $\lambda_{\text{em}} = 465\text{nm}$ for AMC and $\lambda_{\text{ex}} = 488\text{nm}$ and $\lambda_{\text{em}} = 530\text{nm}$ for FITC.

SARS-CoV-2 infection and protease activities

All experiments with SARS-CoV-2 propagation were performed in biosafety level 3 containment laboratories at the University of New Mexico Health Science Center (UNM HSC) with approved protocols.

Optimal infection time and virus concentration. VeroE6 cells (ATCC, Manassas, VA, USA, Cat# CRL-1586) were grown to 90% confluency (approx. 3×10^5 cells per well) in a 12-well plate with Dulbecco's minimal essential medium (DMEM) supplemented with 10% fetal calf serum (FCS) and 1% penicillin/streptomycin. Cells were infected with 0.1 or 0.01 MOI of the SARS-CoV-2 isolate USA-WA1/2020 (BEI Resources, Manassas, VA, USA) in viral growth medium (MEM + 2.5% heat inactivated fetal calf serum) and incubated at 37°C in a humidified incubator for 2, 4, 8, and 24 hours. After each incubation time, cell-based protease assays were performed as described below.

Cell-based PLpro inhibition assays. The well-characterized PLpro inhibitor GRL0617 (R&D Systems) was diluted in MEM without fetal calf serum to achieve concentrations between 2μM-100μM and 100μl was added to near confluent VeroE6 cells in wells of a 24-well plate. Cells were incubated for 2 hours at 37°C in a humidified incubator, washed with 1x PBS, and 0.01 MOI of SARS-CoV-2 USA-WA1/2020 was added in viral growth medium (MEM + 2.5% heat inactivated fetal calf serum). Controls included medium with SARS-CoV-2 with and without DMSO (1% for a final concentration of 0.25%) and medium only with and without DMSO. Cells were incubated at 37°C in a humidified incubator for 24 hours. Cell-based protease activity assays were performed as described below.

Neutralization assays. Patient serum was diluted 1:40, 1:160, 1:640 and 1:1250 in viral growth media (MEM + 2.5% heat inactivated fetal calf serum) and 200μl was added to an equal volume of 0.01 MOI SARS-CoV-2 USA-WA1/2020 in viral growth medium for 2 hours. Controls were medium with SARS-CoV-2 without serum and medium without virus. The mixtures (400μl) were added to 90% confluent VeroE6 cells in 12-well plates and the cells were incubated at 37°C in a humidified incubator for 24 hours. Cell-based protease assays were performed as described below.

SARS-CoV-2 protease activity assays. After cells were incubated with virus for 6–24 hours, the media was removed from the wells and cells washed three times with 100 mM HEPES. Lysis buffer (100μl, Mesa Photonics) was added to each well, incubated for 5 minutes at room temperature and 25μl of lysates added to duplicate wells of a 96 well black plate (Corning). Peptides (25μl) in 2x assay buffer (100mM HEPES, 10mM DTT, pH 7.4) were added to the wells to achieve final concentrations of 2μM DEVD₂-AMC and 50nM Pun74-R110. Fluorescence was read immediately and every 15 minutes for 1 hour in a fluorescence plate reader (Synergy H1, Agilent) with a 3 second shake between reads using $\lambda_{\text{ex}} = 365\text{nm}$ and $\lambda_{\text{em}} = 465\text{nm}$ for AMC and $\lambda_{\text{ex}} = 485\text{nm}$ and $\lambda_{\text{em}} = 528\text{nm}$ for R110.

Host cell lysis and SARS-CoV-2 inactivation by lysis buffer

All experiments determining the lysis of host cells and inactivation of SARS-CoV-2 using Mesa Photonics proprietary lysis buffer were performed in biosafety level 3 containment laboratories at MicroBiologics (MBL, St. Cloud MN) with approved protocols.

Host cell cytotoxicity testing. The ability of the lysis buffer to disrupt mammalian cell membranes was assessed by scoring the lysis buffer-caused morphological changes of VeroE6 cells and by measuring the effect of the lysis buffer on cell viability using the alamarBlue

(Invitrogen) cell viability fluorescence staining reagent. Lysis buffer was used directly or filtered through Pierce detergent removal spin columns (PDRSC) according to the manufacturer's recommendations (Thermo Fisher). 1:10 dilutions of lysis buffer with or without filtration by PDRSC and diluent (water) were prepared in viral growth media (VGM; 2% FBS in MEM with sodium pyruvate, non-essential amino acids, and antimycotic). Vero E6 cells (MBL) were grown in 6-well plates to 90% confluency in cell maintenance media (DMEM with 10% FBS, sodium pyruvate, and non-essential amino acids). The medium was replaced with 500 μ L of fresh VGM and then 100 μ L of lysis buffer dilutions or water were added. To mimic the binding step in plaque assays, the plates were incubated with shaking for 2 hours, the inoculates removed and replaced with 3mL fresh VGM. Cells were observed under an inverted microscope and then the plates were incubated at 37°C (5–6% CO₂). After 7 days, the cell morphology was assessed by microscopy. For viability staining, VGM was removed from each well and replaced with 1mL of 10-fold diluted alamarBlue reagent prepared in VGM. After 4 hours incubation at 37°C, 100 μ L from each well were transferred to wells in a 96-well microtiter plate with flat and clear bottoms (Greiner, cat # 655801). Fluorescence signals were measured using a SpectraMax iD5 microtiter plate reader (Molecular Devices, Sunnyvale, CA) using excitation and emission wavelengths of $\lambda_{\text{ex}} = 560\text{nm}$ and $\lambda_{\text{em}} = 590\text{nm}$.

Virus inactivation testing using plaque assay. Viral inactivation was determined using SARS-CoV-2 stocks from 2 different lots of isolate USA-WA1/2020 virus (BEI NR- 52281/Lot#: 70036318). For the virus only control group, viruses were prepared at 1:10 serial dilutions in VGM. For the experimental group, the viral stock was added to lysis buffer in a ratio of 1:9 and 1:10 serial dilutions prepared in VGM. The remaining infectivity in each sample dilution was determined using plaque assay in 1-day-old VeroE6 monolayer cultures ($\geq 90\%$ confluency) prepared in 6-well cell culture plates. Briefly, cell maintenance medium was removed from the plated cells, and 500 μ L of VGM was added to each well. Then, 100 μ L of test dilutions were added to the corresponding wells. The plates were incubated under slow-speed shaking for 2 hours for virus-cell binding, then the inoculates were removed and 3mL of VGM contain 1.5% or 3% carboxy methyl cellulose (CMC; Teknova, Hollister, CA) were added followed by incubation at 37°C for 5–7 days in a CO₂ Incubator. After incubation, the CMC overlay layer was aspirated and the cell monolayers were fixed by addition of 3mL/well of 10% formaldehyde followed by a 30 min incubation. After removal of the formaldehyde, 2mL of 0.1% Crystal Violet stain solution (Thermo Scientific) was added to each well for 10 minutes. The excess Crystal Violet was rinsed out with deionized (DI) water and the formed plaques were counted to calculate the retained infectivity titer.

SARS-CoV-2 protease assays using human specimens

Ethical approval. This project was approved by the University of New Mexico Health Sciences Center Human Research Protection Program. Review and approval were obtained from the UNM Institutional Review Board (IRB) under Study Numbers 22–373 and 22–038. All relevant ethical guidelines and regulations were followed, and study participants provided written informed consent. None of the subjects were taking antivirals and were directed to refrain from smoking, chewing tobacco, eating, or drinking 60 minutes prior to specimen collection.

SARS-CoV-2 PLpro activity assays in lysates from tongue scrape and saliva. The study entitled “A new, Simple On-Site Test for Detection of SARS Coronaviruses” compared the performance of the SARS-CoV-2 PLpro protease assay between lysates obtained from saliva and tongue scrape specimens.

Study population. 14 male and 9 female subjects were enrolled between May 23, 2022 and June 23, 2022 after presenting to the Emergency Department with clinical signs of

respiratory disease. COVID-19 was confirmed or ruled out by RT-PCR using a diagnostic standard of care test that had been approved under the FDA Emergency Use Authorization Framework (Cobas LIAT RT-PCR using nasopharyngeal swabs). 13 patients with positive and 10 patients with negative RT-PCR results were enrolled in the study.

Tongue scrape specimens were obtained by gentle and painless scraping of the tongue three times from back to front using a disposable tongue cleaner (Grin Oral Care, San Diego, CA). Tongue cleaners together with the adhering samples were placed in 50mL flat bottom sample collection tubes (Environmental Express), and 1mL 2x lysis buffer was added using a 1mL transfer pipette (Sigma Aldrich, St. Louis MO).

Saliva specimens were obtained by passive drooling through a straw. Raw saliva was transferred to a vial containing 200 μ L 2x lysis buffer using a 200 μ L Samco™ Exact Volume Transfer Pipette (Thermo Scientific).

Lysates were briefly vortexed and 200 μ L transferred to a Reaction Vial containing freeze dried assay components in a 0.5mL PCR Tube (Promega, Madison, WI) for final concentrations of 5mM DTT, 50mM HEPES, 20 μ M PLpro peptide Pun16-AMC, and 20 μ M caspase peptide DEVD₂-R110. In addition, 200 μ L lysate was transferred to a separate vial (QuantiVial) containing the nucleic acid intercalating “Quanti dye”. Reaction Vials were inserted into a PCR tube adapter (Promega, E6101) and the fluorescence measured in a battery-operated fluorometer (Turner Designs, San Jose, CA) with 2 channels configured for dual fluorescence measurements: Channel A = UV LED, 365nm excitation filter, 440/15nm emission bandpass filter was used to measure fluorescence from the PLpro peptide Pun16 labeled with AMC. Channel B = Blue LED, 475nm excitation filter, 515/10nm emission bandpass filter was used to measure fluorescence from the internal control peptide DEVD₂-R110. Fluorescence from the Reaction Vial was measured immediately (time 0) and every 30 minutes for 1 hour (time 60) in both channels. The fluorescence from the QuantiVial was measured once after 1 hour in Channel B. Values were recorded manually and the difference between relative fluorescence units (RFU) measured at time 60 and time 0 calculated (delta RFU). The delta RFU were normalized for the amount of material collected using the RFU measured in the QuantiVial according to the formula (Delta RFU protease/RFU QuantiVial)*100.

SARS-CoV-2 PLpro / MPro assays in lysates from saliva specimens

A second study entitled “A new, Simple On-Site Test for Detection of SARS Coronaviruses in Saliva” compared the performance on saliva that was split for the SARS-CoV-2 protease assays and for RT-PCR on purified RNA.

Study population. 9 male and 13 female subjects were enrolled between June 6, 2023, and September 27, 2023, who presented to the Emergency Department with symptoms consistent with COVID-19. A positive or negative RT-PCR diagnosis was made using standard of care Cobas LIAT RT-PCR on nasal mid-turbinate (NMT) swabs. None of the subjects were taking antivirals and were directed to refrain from smoking, chewing tobacco, eating, or drinking 60 minutes prior to specimen collection.

Saliva specimens (500 μ L) were collected using a SpeciMAX™ Saliva Collection kit (Thermo Scientific, Waltham, MA). For the protease tests, 200 μ L lysate was added to vials containing 200 μ L 2X Lysis buffer (Mesa Photonics). In this study, SARS-CoV-2 PLpro and MPro protease assays were performed in 384-well plates and the fluorescence monitored in a fluorescence plate reader. In three separate experiments, lysate (10 μ L) was added to triplicate wells and reactions started by addition of 10 μ L reaction mixtures. Reaction mixtures contained A) the MPro-R110 peptide and B) the PLpro peptide Pun16-R110 to yield final concentrations of 2 μ M peptide in 5mM DTT and 50mM HEPES, pH 7.4; C) a 2.5x dilution of Quanti dye was added to

separate triplicate wells containing lysate. Fluorescence was monitored every 2 minutes in a fluorescence plate reader for 30 minutes using $\lambda_{\text{ex}} = 485\text{nm}$ and $\lambda_{\text{em}} = 528\text{nm}$ at 30°C .

Data analysis. For MPro assays, the delta RFU was calculated from the difference in relative fluorescence units (RFU) measured immediately and after 30 minutes and for PLpro assays, the delta RFU was calculated from the difference in RFU measured between 10 and 30 minutes. The coefficient of variation (CV) was calculated using the formula: (standard deviation / mean of RFU from triplicate values)*100. The Delta RFU were normalized for the amount of sample collected by calculating the ratio between the RFU from the protease assays and Quanti dye using the formula (Delta RFU Protease assay/RFU Quanti dye)*100. The ratio of CV was calculated using the formula $Ratio\ CV = \sqrt{(CV_{PLpro}^2 + CV_{QV}^2)}$. Pearson correlations were determined using GraphPad Prism software version 10.2.0 (Boston, MA).

The amount of lysate required to detect MPro and PLpro activities was determined by calculating the lysate concentrations at which positive and negative specimens no longer produced different results. Serial dilutions of lysates from patients who tested positive or negative for SARS-CoV-2 by RT-PCR were prepared in lysis buffer and peptides added for 30 minutes (S1 Fig). Quanti Dye was added to lysate in separate wells. For MPro and PLpro, the slopes and y intercepts were determined by linear regression using GraphPad Prism. The concentration of lysate on the x-axis from positive (b2) and negative (b1) specimens were calculated using the formula $x = (b_2 - b_1) / (m_1 - m_2)$, where b is the y intercept and m is the slope. Interpolation of these values to the linear fit from the Quanti Dye RFU was performed using the formula $y = mx + b$.

The cutoff value for PLpro test positivity was determined by dividing the mean values of the slopes of the PLpro reactions in various lysate dilutions by the slope of Quanti Dye from various lysate dilutions (S1 Fig) and multiplying by 100. The positive cutoff value for PLpro was determined as 27.7.

Reverse transcription and polymerase chain reaction

RNA Isolation. Saliva (200 μl) from the same specimen used for the protease assays was transferred to a vial containing an equal volume of RNA Shield (Zymo Research, Irvine, CA). RNA was isolated using the Zymo Research Quick-DNA/RNA Viral Kit according to manufacturer's recommendations. SARS-CoV-2 RT-LAMP and TaqPath One step RT-PCR were performed as described below.

SARS-CoV-2 RT-LAMP. Loop-mediated isothermal amplification (LAMP) RT-PCR was performed using the SARS-CoV-2 Rapid Colorimetric LAMP Assay Kit from New England Biolabs (Ipswich, MA) according to the manufacturer's instructions with the supplied primers that target the SARS-CoV-2 nucleocapsid (N) gene, the envelope (E) gene, and the internal control actin. LAMP Fluorescent Dye (NEB) was added at a 1x final concentration to enable real-time fluorescence monitoring. The reactions were prepared in Fast Reaction Tubes with Cap (Thermo Fisher), overlaid with 20 μl mineral oil, and incubated for 30 minutes at room temperature. Tubes were placed in an AXYGEN PCR Tube Storage Rack (#80086-082, Corning, NY) and the rack inserted into a Synergy H1 fluorescent plate reader using the following plate settings: Biotek PCR adapter 2 cm plate, bottom read, read height 7 mm. Fluorescence was measured every 2 minutes for 60 minutes at 65°C in kinetic mode using excitation and emission wavelengths of $\lambda_{\text{ex}} = 485\text{nm}$ and $\lambda_{\text{em}} = 528\text{nm}$.

Endpoint SARS-CoV-2 RT-PCR. The TaqPath™ 1-Step Multiplex Master Mix (no ROX, Thermo Scientific) was used to amplify 2 μl RNA according to the manufacturer's instruction for FAST cycling. Primers for SARS-CoV-2 N1, N2, and RNase P genes were purchased from Integrated DNA Technologies (Coralville, IA). The sequences correspond to those supplied with the 2019-nCov CDC EUA Kit [45].

Reactions (20 μ l) were prepared in 0.2mL PCR tubes, overlaid with mineral oil, and RT-PCR performed in a MiniAmp Thermocycler (Thermo Fisher) using thermal cycling conditions of 2 minutes at 25°C (UNG incubation), 10 minutes at 53°C (reverse transcription), 2 minutes at 95°C (polymerase activation) and 40 cycles of 3 seconds at 95°C and 30 seconds at 60°C.

1.5 μ l Safestain 6x DNA Loading Dye (Lambda Biotech, St. Louis, MO) was added to 8 μ l PCR products and 10 μ l (0.8 μ g) 100 bp DNA Ladder (Lambda Biotech) or to 1 μ g 50 bp DNA Ladder (New England Biolabs). Samples (8 μ l) were loaded into wells of a 2% agarose gel and electrophoresis performed for 1–2 hours at 40 Volts (~1 Watt) in Tris Borate EDTA (TBE) buffer. Peak intensities of the bands were quantified using ImageJ and the percentage of SARS-CoV-2 amplicon intensities calculated relative to the intensities of the RNase P amplicons [46].

Results

Relative fluorescence units (RFU) for the results shown are reported in the supporting file (S1 File).

Detection of mono-ubiquitin and ISG15 cleavage in lysates from human-infecting coronaviruses

Papain-like proteases are expressed by other human coronaviruses (hCoV)—SARS-1, MERS, NL63, OC43, HKU1 and 229E—that also cleave the LRGG sequence in reporter substrates. To determine whether the PLpro assay was sensitive enough to detect papain-like protease activities in cell-based assays, we first tested human coronaviruses that could be grown in a biosafety level 2 laboratory. Papain-like proteases from both non-SARS-CoV-2 human-infecting coronaviruses and SARS-CoV-2 PLpro reportedly have deubiquitinating (DUB) and deISGylating activities with high enzymatic efficiencies [44, 47]. Accordingly, in our *in vivo* PLpro assay, we were able to detect cleavage of ISG15-AMC in lysates from approximately 24,000 human MRC-5 and HCT8 cells infected with the human coronaviruses 229E and OC43, respectively. Mono ubiquitin-AMC cleavage was detectable after 15 minutes in lysates from LLC-MK2 cells that were infected with NL63 (S2 Fig) but we were unable to observe stable signals from tetrapeptide cleavage in any of the lysates tested.

Peptides with improved sensitivity and specificity of detection

In a next step, we aimed to combine the observed sensitivity of detection by using peptides containing sequences of ISG15, which PLpro is known to cleave with >7,800 higher efficiency than the tetrapeptide alone, with specificity of detection required for a SARS-CoV-2 diagnostic test [44]. Specificity was conferred by incorporating unnatural amino acids into the PLpro cleavage site following Rut et al., who showed that PLpro from SARS-1 and SARS-CoV-2 have unique preferences for amino acids in the LXGG cleavage sequence (where L = leucine at position 4, X = any amino acid at position 3, G = glycine at position 2, and G = glycine at position 1). They found that only glycine is accepted at positions 1 and 2, a broad range of amino acids are accepted at position 3, and hydrophobic residues only are accepted at positions 4 [48]. We therefore synthesized peptides containing 16 or 74 amino acids from ISG15 and unnatural amino acids in the cleavage site (Pun16 and Pun74).

The increased detection sensitivity of the longer peptide relative to the tetrapeptide P4-AMC was estimated in a biochemical assay by determining the concentration of recombinant PLpro required to produce a half maximum signal (EC_{50}). The tetrapeptide P4-AMC did not saturate the enzyme at the highest concentration tested and the EC_{50} was estimated as half

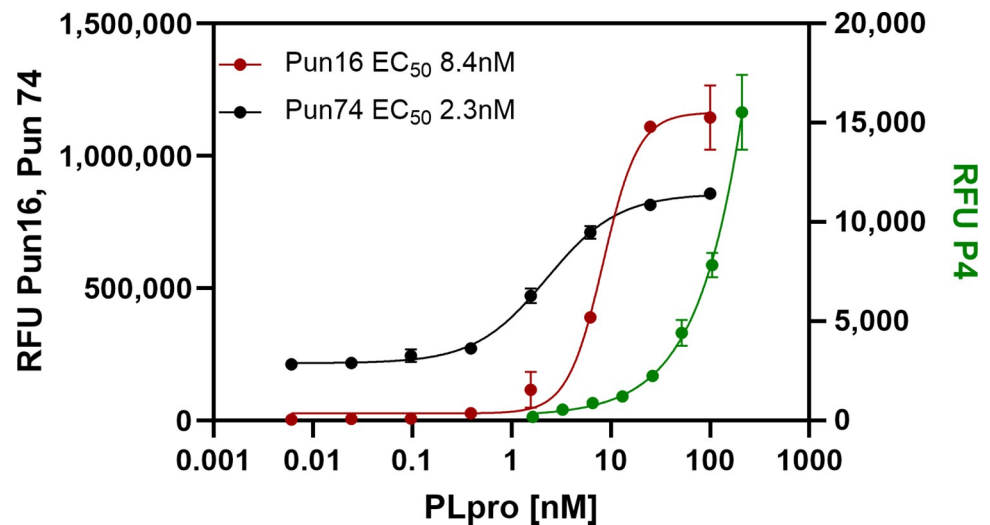


Fig 2. Effect of PLpro peptide length on detection sensitivity. A serial dilution of recombinant PLpro was prepared in assay buffer and added to duplicate wells of a 384-well plate. Peptides in assay buffer were added and the plate incubated for 60 minutes at room temperature. The final concentration of Pun74-R110 was 300nM and 30 μ M for P16-AMC and P4-AMC. Fluorescence was monitored using dual wavelength monitoring for R110 (λ_{ex} = 485nM and λ_{em} = 528nM) and AMC (λ_{ex} = 365nM and λ_{em} = 465nM). Error bars represent standard deviations of the mean relative fluorescent units (RFU) from duplicate wells.

<https://doi.org/10.1371/journal.pone.0309305.g002>

the signal after 1 hour of incubation (EC_{50} = 100nM). This resulted in an estimated 12 and 43.4-fold increase in detection performance for a 16-mer peptide (Pun16-AMC; EC_{50} = 8.4nM) and 74-mer peptide (Pun74-R110; EC_{50} = 2.3nM) (Fig 2).

Next, we tested cleavage of the ISG15-based peptide Pun16-AMC that contained unnatural amino acids at positions 4 and 3 by recombinant papain-like proteases from other human pathogens known to have deISGylating activities. Fig 3 shows that Pun16-AMC was significantly cleaved by recombinant PLpros from SARS-1 and SARS-CoV-2 but not by recombinant papain-like proteases from the other five human coronaviruses, by the human deISGylating enzyme USP18, or Adenovirus L3. We verified that all recombinant papain-like proteases were catalytically active by measuring the RFU resulting from cleavage of positive control substrates that contained only natural amino acids in the cleavage sites. The positive control peptide P16-AMC has the same amino acid sequence as Pun16-AMC but with the natural amino acids leucine (L) and arginine (R) in the cleavage sequence. P16-AMC was cleaved by recombinant papain-like proteases from SARS-1, SARS-CoV-2, NL63, MERS, and 229E but not by papain-like proteases from OC43 and HKU1; for these enzymes, ubiquitin-AMC was used as the positive control substrate instead. The positive control substrate for USP18 was human ISG15-R110, and the positive control substrate for the adenovirus L3 protease was the tetrapeptide P4-AMC (Fig 3).

The study with recombinant enzyme showed that the PLpro peptide Pun16-AMC with unnatural amino acids in the cleavage site was strongly cleaved by PLpros from SARS-1 and SARS-CoV-2 (73.7% and 46.9% relative to P16-AMC, respectively), minimally cleavage by PLPs from HCoV NL63 and 229E (12.1% and 3.7% relative to P16-AMC, respectively), and not detectably cleaved by the other proteases tested. The lack of cross-reactive cleavages supported the expectation that cleavage activities measured in crude lysates would be predominantly from SARS-CoV-2 PLpro and not from proteases of other human coronaviruses or endogenous proteases that may be present in lysates.

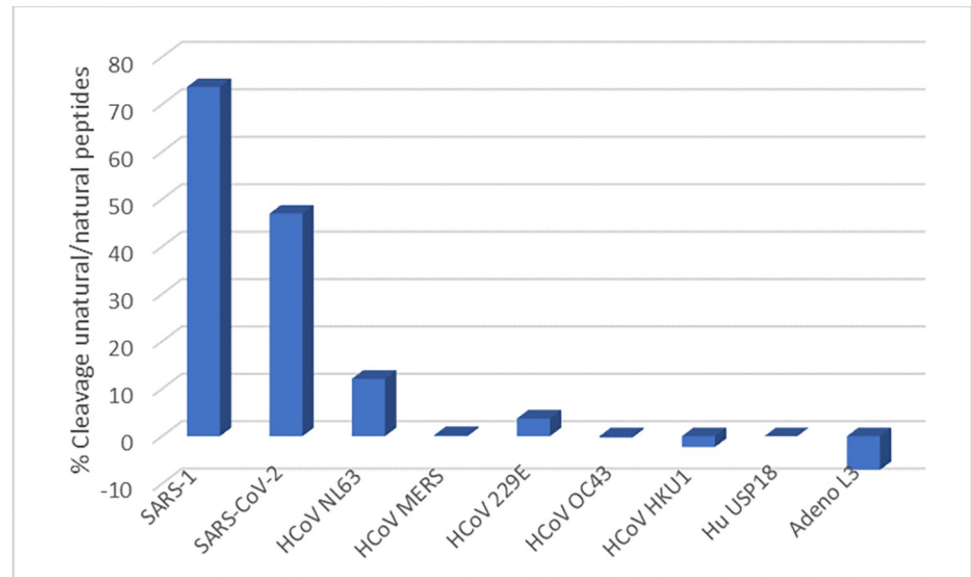


Fig 3. Cleavage of PLpro peptide Pun16-AMC by various papain-like proteases. The fluorescence from the cleavage of PLpro peptide Pun16-AMC with unnatural amino acids in the cleavage site and from the cleavage of positive control substrates with natural amino acids was measured. The concentrations of papain-like proteases were 100nM (SARS-1, SARS-CoV-2), 250nM (Adenovirus L3), 1200nM (MERS, 229E, HKU1, USP18), and 1760nM (OC43). The concentration of positive control substrate P16 was 25 μ M for papain-like proteases from SARS-1, SARS-CoV-2, NL63, MERS, 229E, and 10 μ M Ubiquitin-AMC for papain-like proteases from OC43 and HKU1, 0.5 μ M ISG15-R110 for USP18 and 60 μ M P4 for adenovirus L3 protease. The reaction progress was monitored for 60 minutes at room temperature and the differences in RFU between time 60 and time 0 calculated (delta RFU). The percent cleavage activity of peptide Pun16-AMC was calculated relative to the delta RFU of the control substrates ($(\text{delta RFU}_{\text{control}} / \text{delta RFU}_{\text{Pun16}}) * 100$).

<https://doi.org/10.1371/journal.pone.0309305.g003>

Detection of PLpro and caspase activities in crude lysates from SARS-CoV-2 infected VeroE6 cells

Next, we tested whether the PLpro Pun peptides, which were designed and optimized for cleavage by SARS-CoV-2 PLpro *in vitro*, could produce fluorescent signals in crude lysates from SARS-CoV-2 infected VeroE6 cells that could be discriminated from background fluorescence produced by potential host cell protease cleavage. When lysates from 3×10^5 VeroE6 cells were tested that were infected with a multiplicity of infection (MOI) of 0.1, we observed strong fluorescent signal increases predominantly in lysates from infected cells and not in those from uninfected cells that were run in parallel as a control (Fig 4, left). After 60 minutes of incubation with Pun74-R110, the ratio of RFU at 60 minutes/RFU at time 0 (Signal to Background) from infected cell lysates was 16 while the S/B from uninfected cell lysates was only 1.8. This demonstrates that 90% of the measured fluorescence resulted from cleavage of the PLpro peptide Pun74-R110 by PLpro rather than from endogenous proteases present in the lysate. Interestingly, we were able to detect PLpro activity in lysates from VeroE6 infected cells only with the PLpro peptide Pun74-R110, which is based on mouse ISG15, while none of the peptides that are based on the human ISG15 sequence performed (data not shown).

We also measured the fluorescence resulting from the cleavage of the peptide with the sequence DEVD, which is recognized by caspases, and determined that this peptide can be used as an internal processing control to confirm that lysates were present in sufficient quantity and quality for the assay to perform. As expected, infected cells demonstrated higher cleavage of the DEVD peptide than uninfected cells as the cleaving enzymes, caspases, are upregulated in pathogen-infected cells preparing to undergo apoptosis (Fig 4) [49].

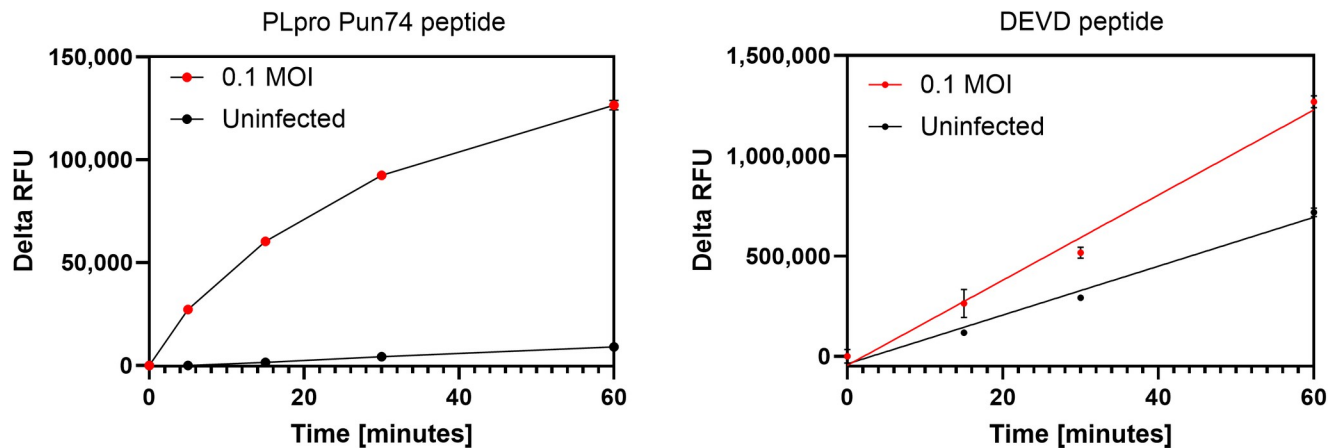


Fig 4. Fluorescence increases from cleavage of PLpro and DEVD peptides by SARS-CoV-2 PLpro and caspases in crude lysates from SARS-CoV-2 infected VeroE6 cells. VeroE6 cells (3×10^5) were infected with 0.1 MOI SARS-CoV-2 for 12 hours and lysates prepared from infected (red traces) and uninfected (black traces) cells. Lysates (25 μ l) were added to wells of a 96-well plate and 25 μ l of peptide in 2x assay buffer added. **Left.** PLpro peptide Pun74-R110 (50nM) or **Right** DEVD₂-R110 (2 μ M). The increase in relative fluorescence units (RFU) in x2 replicates was monitored immediately and after every 15 minutes for 60 minutes at room temperature in a fluorescence plate reader using excitation and emission wavelengths of $\lambda_{ex} = 485\text{nm}$ and $\lambda_{em} = 528\text{nm}$. RFU were plotted using GraphPad Prism software. Some error bars are within the symbols. Pun74 substrate depletion in lysates from infected cells resulted in non-linear fluorescence increases after approximately 15 minutes. The results were reproducible in five separate experiments.

<https://doi.org/10.1371/journal.pone.0309305.g004>

Time course of PLpro activity in lysates from SARS-CoV-2 infected VeroE6 cells. To determine the optimal incubation time and multiplicity of infection (MOI) for detecting SARS-CoV-2 PLpro activity, we incubated SARS-CoV-2 at MOIs of 0.1 and 0.01 with VeroE6 cells and prepared lysates after various incubation times. The PLpro peptide was added to the lysates and the S/B was calculated between the start of the reaction and after 60 minutes of incubation (Fig 5). We found that lysates infected with an MOI of 0.1 produced a S/B of 12 after 6 hours of incubation, which was approximately 2.4 times greater than the S/B of 5 that was obtained in lysates from uninfected cells. These results correspond to the reported detection of intracellular SARS-CoV-2 virions ~10 hours post infection which require PLpro activity for assembly [31]. In contrast, lysates from cells that were infected with an MOI of 0.01 required an incubation time of approximately 24 hours to achieve a noticeable difference relative to uninfected cells (S/B of 27 versus 4.9). Although the experiment was performed only once, the results suggest that assays can be completed within 1 working day from infection to result using an MOI of 0.1, or in 2 working days using an MOI of 0.01 with a 24-hour incubation (Fig 5).

Measurement of PLpro inhibition in crude lysates from SARS-CoV-2 infected VeroE6 cells. The excellent performance of the PLpro assay in crude lysates from VeroE6-infected cells encouraged us to test whether the platform has potential for use as a screening tool to identify PLpro inhibitors. Feasibility was demonstrated using the well characterized PLpro inhibitor GRL0617 [50]. For the inhibition assay, various concentrations of inhibitor were added to VeroE6 cells and incubated for 2 hours. SARS-CoV-2 was added at an MOI of 0.01 for 24 hours, after which protease activities were measured as described. The results shown in Fig 6A demonstrate that a concentration of 100 μ M of the inhibitor GRL0617 reduced the fluorescence to nearly the background fluorescence of the wells containing lysates from uninfected and untreated cells (medium only or medium + DMSO no virus), while lower concentrations of inhibitor caused only a slight decrease in fluorescence relative to lysates from infected cells (medium + virus).

The tentative IC_{50} value of 38.3 μ M obtained for GRL0617 in our hands was within one order of magnitude of the $EC_{50} = 21 \pm 2 \mu\text{M}$ reported in a virus proliferation assay,

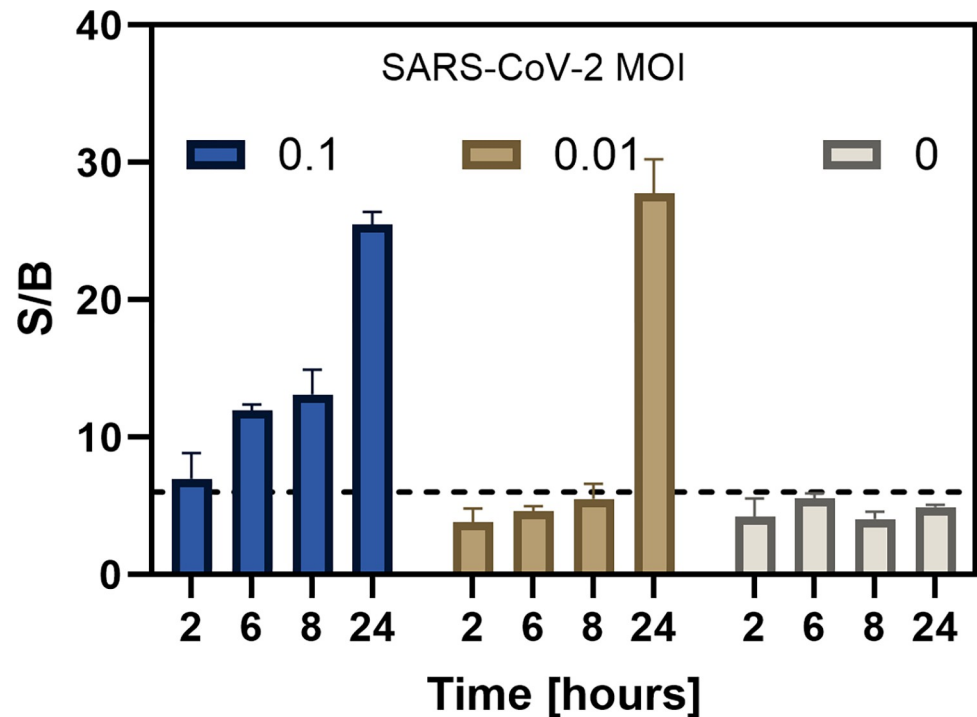


Fig 5. Time course of fluorescence increases in lysates from VeroE6 cells infected with SARS-CoV-2. VeroE6 cells (~300,000 cells per well) were plated in a 12-well plate. 4 wells were infected with a MOI of 0.1 or 0.01. Control cells were not infected and treated with medium. Lysis buffer (100 μ l) was added to washed monolayers and 25 μ l of lysates (corresponding to 75,000 cells) from each time point were combined with the PLpro substrate Pun74-R110 in wells of a 96-well plate. The increases in relative fluorescence units (RFU) were measured in x2 replicates immediately and after 60 minutes in a fluorescence plate reader using excitation and emission wavelengths of $\lambda_{ex} = 485\text{nm}$ and $\lambda_{em} = 528\text{nm}$. The ratio of RFU between the 60-minute read and the initial read was calculated and plotted as Signal to Background (S/B) using GraphPad Prism software. A S/B of 6 was used as a cutoff and is indicated by a dotted line.

<https://doi.org/10.1371/journal.pone.0309305.g005>

demonstrating successful inhibition. Although this experiment was performed only once with 2x replicates, the results suggest that the assay can be used for rapid screening of PLpro inhibitors against endogenous PLpro (Fig 6) [50].

Detection of serum neutralizing activities using SARS-CoV-2 PLpro as a marker of infection. A neutralization assay was performed to determine whether PLpro activity can be used as a marker of infection and determine the neutralizing activity of anti-SARS-CoV-2 antibodies. Building on the information gained from the time point experiment (Fig 5), we conducted a neutralization assay in which a MOI of 0.01 SARS-CoV-2 was combined for 2 hours with various dilutions of anti-SARS-CoV-2 positive serum. This mixture was then added to VeroE6 cells and lysates were prepared after 24 hours of incubation. The cell-based protease assay was performed as described and the delta RFU calculated after 30 minutes. Lysates from cells that were challenged with virus pretreated with serum dilution from 1:40, 1:160, and 1:640 produced fluorescence that was not distinguishable from the delta RFU obtained from uninfected control lysates (Fig 7, Medium), demonstrating complete neutralization. In contrast, lysates from cells in which SARS-CoV-2 had been incubated with the serum dilution of 1:2,560 produced delta RFU that was 33% lower than the delta RFU from untreated virus (Medium + virus), indicating that infection, albeit at a lower level, had occurred. If reproducible, these findings from a single experiment suggest that PLpro cleavage activity is a useful biomarker for rapidly determining antibody neutralization activity (Fig 7).

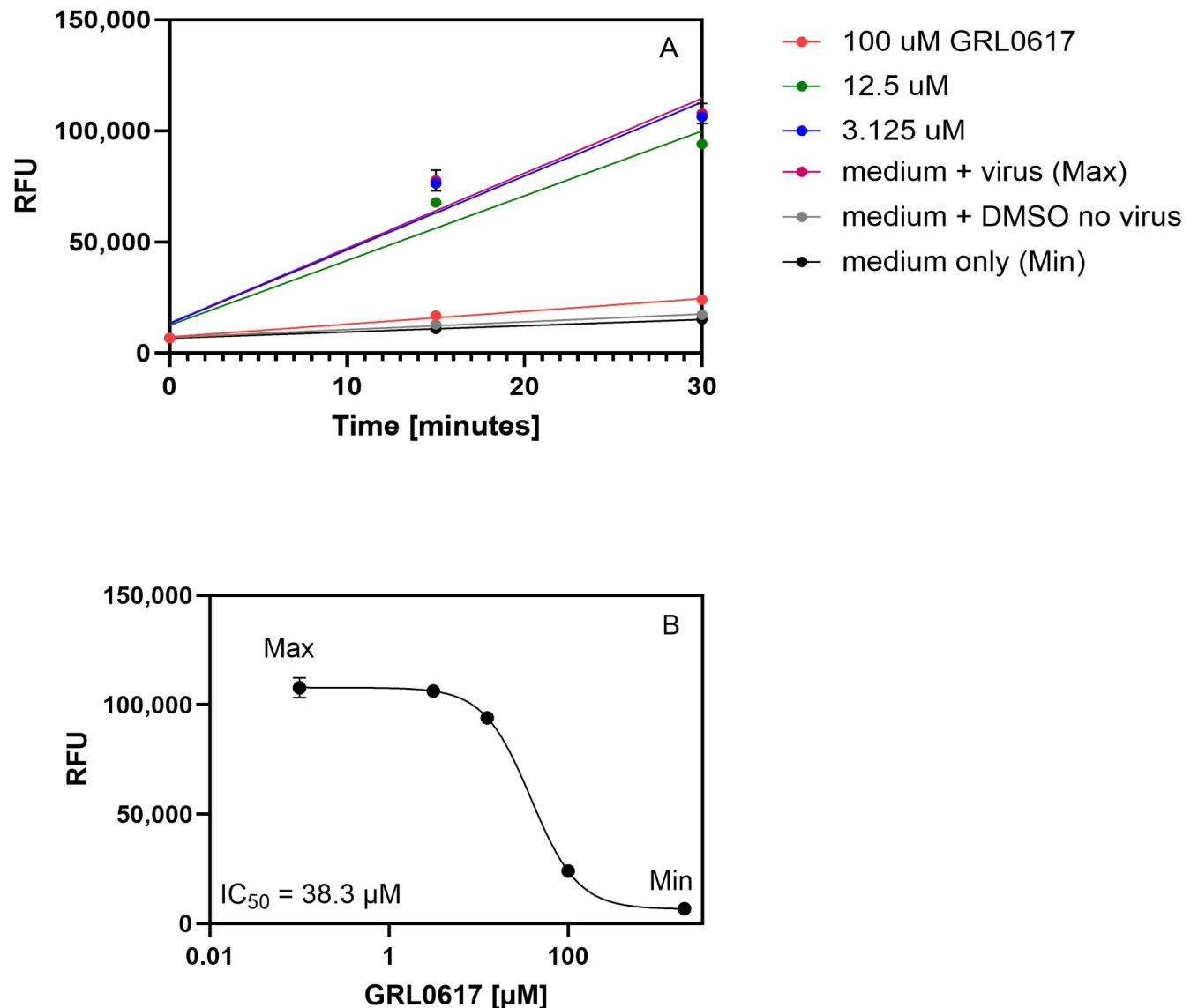


Fig 6. Fluorescence from PLpro peptide cleavage in lysates from VeroE6 cells infected with GRL0617 pretreated SARS-CoV-2. VeroE6 cells were seeded in a 24-well plate and incubated at 37°C for 12 hours. Various dilutions of the inhibitor GRL0617 were prepared in MEM without FCS, added to the cells, and incubated for 2 hours at 37°C. Control cells were uninfected and infected cells treated with medium only and uninfected cells treated with medium plus DMSO. SARS-CoV-2 (0.01 MOI) was added for 24 hours at 37°C and lysates prepared. PLpro substrate Pun74-R110 was added in 2x assay buffer and 25µl added to wells in a 96-well plate for a final concentration of 50nM. **A**) The increase in relative fluorescence units (RFU) from Pun74 cleavage in x2 replicates was monitored every 15 minutes for 30 minutes at room temperature in a fluorescence plate reader using excitation and emission wavelengths of $\lambda_{ex} = 485\text{nm}$ and $\lambda_{em} = 528\text{nm}$. **B**) The mean RFU after 30 minutes in lysates from cells pretreated with GRL0617, from untreated infected cells (medium plus virus (MAX RFU)), or from uninfected cells (medium without virus (MIN RFU)) were plotted and the IC₅₀ calculated using GraphPad Prism, nonlinear regression, variable slope. Some error bars are within the symbols.

<https://doi.org/10.1371/journal.pone.0309305.g006>

Host cell lysis and SARS-CoV-2 inactivation by Mesa Photonics lysis buffer

Handling of infectious SARS-CoV-2 is currently restricted to high-containment laboratories, but specimens can be handled at a lower containment level if virus is inactivated. The lysis buffer used for all experiments performed here is a proprietary mixture of detergents that do not interfere with the activities of the enzymes tested but is expected to disrupt the lipid membranes of host cells and virus, thus inactivating SARS-CoV-2. Complete host cell lysis was

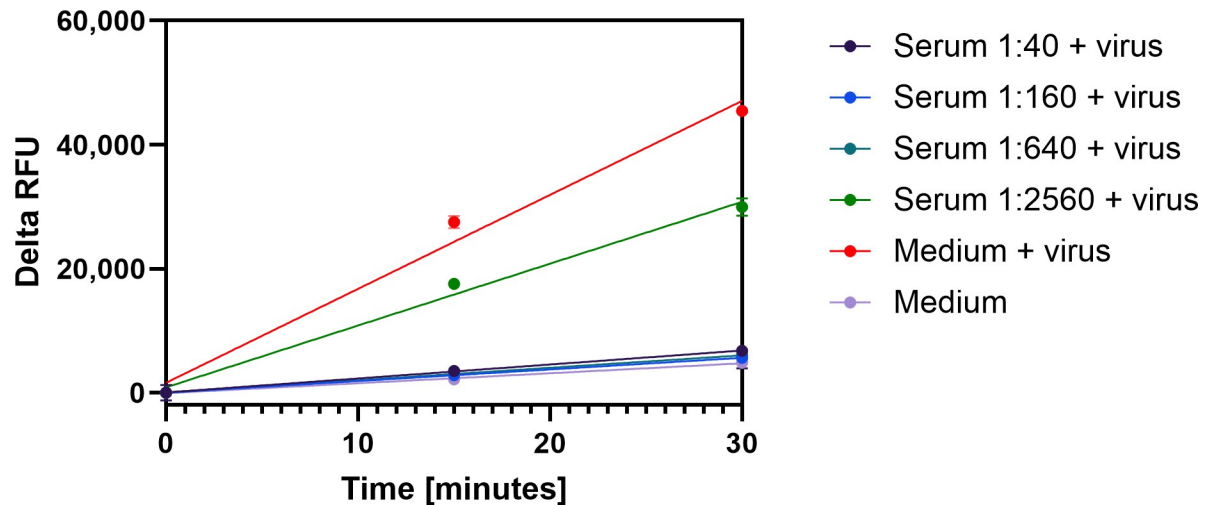


Fig 7. Fluorescence from PLpro peptide cleavage in lysates from VeroE6 cells infected with serum pretreated SARS-CoV-2. VeroE6 cells were seeded in a 12-well plate and incubated at 37°C for 12 hours. Various dilutions of serum were prepared in viral growth medium and combined with equal volumes of 0.01 MOI of SARS-CoV-2 for 2 hours at 37°C. The mixtures were added to the confluent VeroE6 cells for 24 hours at 37°C. Control cells were uninfected cells treated with medium or infected cells treated with media only. Cells were washed, lysates prepared and transferred (25µl) to duplicate wells of a 96-well plate. PLpro substrate Pun74-R110 was added in 2x assay buffer for a final concentration of 50nM. The increase in relative fluorescence units (RFU) from peptide cleavage was monitored every 15 minutes for 30 minutes at room temperature in a fluorescence plate reader using excitation and emission wavelengths of $\lambda_{ex} = 485\text{nm}$ and $\lambda_{em} = 528\text{nm}$. The difference in RFU between the 30-minute read and the initial read was calculated and plotted as Delta RFU using GraphPad Prism software.

<https://doi.org/10.1371/journal.pone.0309305.g007>

observed by microscopy when VeroE6 cells were treated with a 0.33x concentration of lysis buffer for 5 minutes, whereas 0.033x dilutions did not cause host cell lysis (S3 Fig). The results were quantified by alamarBlue staining, where lysis buffer treated cells exhibited a 2-log reduction in fluorescence signal relative to the control groups (S4 Fig).

Further, complete inactivation of 2 different lots of the SARS-CoV-2 WA strain (V00193 and V00282) was observed by plaque assay following a 5-minute incubation with lysis buffer, even at a 0.033x concentration, thus confirming that lysates containing a 1x dilution of lysis buffer can be safely handled during specimen testing (S5 Fig).

Detection of SARS-CoV-2 PLpro activity in patient saliva and tongue scrape specimens in Point of Care Testing (POCT)

Following the successful demonstration of specific and sensitive cleavage of the PLpro Pun74 peptide in lysates from VeroE6 cells infected with SARS-CoV-2, we aimed to evaluate the performance of the test in lysates from human specimens. We first compared human tongue scrape and saliva specimens, given the reported abundance of epithelial cells on the tongue and in other tissues of the oral cavity that express the ACE2 receptor through which SARS-CoV-2 enters the cell [51–54]. Saliva contains between 2–4 million epithelial cells/mL that are shed into saliva [52]. Having been able to detect protease activities in lysates from 75,000 VeroE6 cells (Fig 5) we hypothesized that the assay would have sufficient sensitivity to detect PLpro and caspase cleavage activities in 100µl saliva, estimated to contain 200,000 to 400,000 potentially infected epithelial cells [52].

Our objective was to compare the performance of the test in lysates derived from tongue scrape specimens and saliva, to determine if one type of specimen had an advantage over the other. We collected paired specimens from a total of 23 subjects who had given their informed

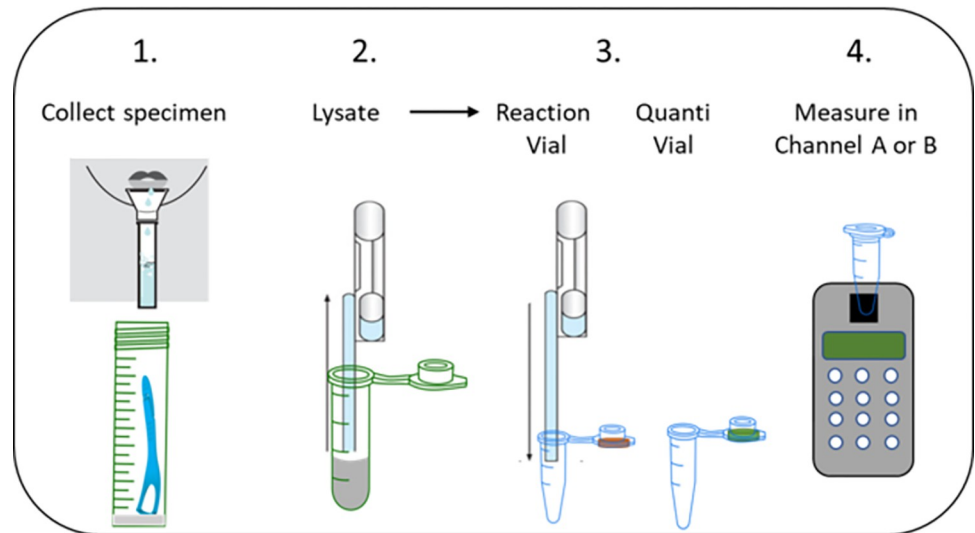


Fig 8. Procedure for measuring SARS-CoV-2 PLpro activity in a Point of Care Testing (POCT) setting. (1) Saliva was collected either through passive drooling using a straw or with a saliva collection device. A volume of 200 μ l of raw saliva was then transferred to a vial containing 200 μ l of 2x Lysis Buffer which immediately lyses cells and inactivates SARS-CoV-2. Painless tongue scrape specimens were collected using a commercial disposable tongue scraper and deposited into a tube containing 1 ml 2x Lysis Buffer. (2) The lysates were transferred using a disposable Exact Pipette and (3) 200 μ l was added to a Reaction Vial that contained lyophilized mixtures of reporter peptides for SARS-CoV-2 PLpro and caspases in assay buffer. An additional 200 μ l of the lysate was transferred to a separate vial containing lyophilized DNA intercalating dye (Quanti Vial) that was used to normalize the fluorescence signal against the amount of sample present. (4) The reaction mixtures were briefly mixed, and the vials inserted into the port of a battery-operated fluorometer that was configured to read fluorescence with excitation and emission wavelengths of $\lambda_{ex} = 360\text{nm}$ and $\lambda_{em} = 460\text{nm}$ (Channel A for PLpro peptide Pun16) or $\lambda_{ex} = 490\text{nm}$ and $\lambda_{em} = 520\text{nm}$ (Channel B for DEVD internal control peptide). Fluorescence from the Reaction Vial was monitored immediately and every 30 minutes for 1 hour and the values recorded manually. Only minor cleavage of the internal processing control peptide DEVD was observed in an uninfected specimen (Fig 9, Example A), whereas cleavage was high in lysates from infected cells undergoing apoptosis (Fig 9, Example C). Therefore, while this peptide was useful to demonstrate active lysates, it could not be used to normalize signals for the amount of sample present. For normalization, we measured the fluorescence from the Quanti Vial in Channel B at the end of the experiment. The normalized delta RFU were calculated using the formula $((\text{RFU}_{t=60} - \text{RFU}_{t=0}) / \text{RFU}_{\text{QuantiVial}}) * 100$.

<https://doi.org/10.1371/journal.pone.0309305.g008>

consent and had been instructed to abstain from eating, drinking, or using tobacco products for 60 minutes prior to specimen collection and had not taken antivirals. The specimens were inactivated by addition of lysis buffer.

Testing was performed by minimally trained operators in a setting closely resembling a Point of Care Testing (POCT) site, using a portable battery-operated fluorometer and vials containing freeze-dried reaction components that did not require refrigeration or special storage conditions. The two-channel fluorometer was configured specifically for our test to enable us to measure the fluorescence produced by the PLpro peptide Pun16 (labeled with AMC) and the internal processing control DEVD peptide (labeled with Rh110) in a single sample vial. Interestingly, the PLpro peptide Pun74-R110 that was used to measure PLpro activity in VeroE6 infected cells did not increase the detection sensitivity in this study or in the second study performed on saliva samples (S6 Fig). These results were reproducible with 6 other specimens.

Fluorescence signals were normalized for the amount of lysate present by measuring the fluorescence from the nucleic acid intercalating dye (QuantiVial) in a separate specimen vial. The steps involved in the measurement process are illustrated in Fig 8.

Lysates from tongue scrapes and saliva specimens were tested in parallel. Examples of a positive result, a negative result, and an inconclusive result are shown in Fig 9.

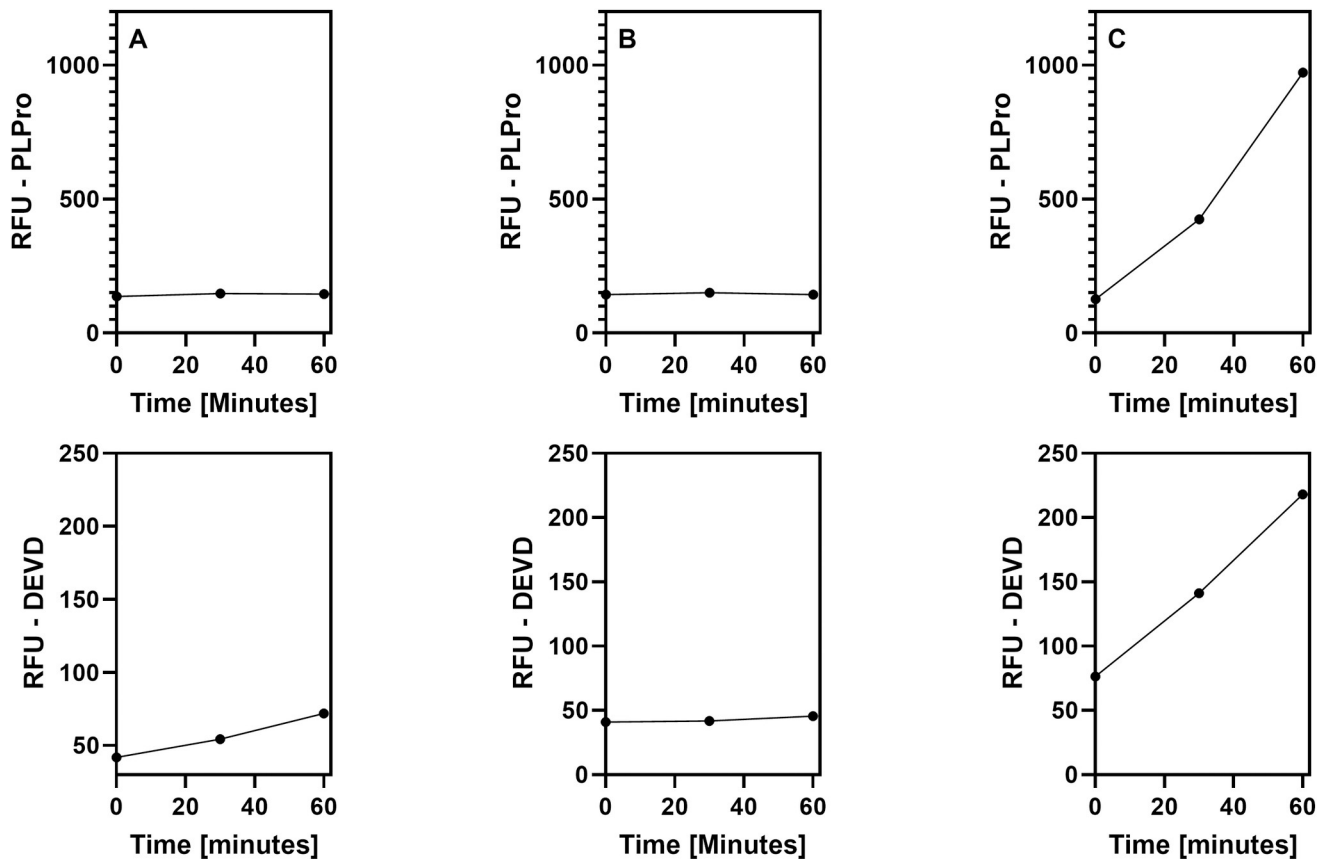


Fig 9. Examples of test results from subject saliva lysates. Specimens were processed as described in Fig 8 and relative fluorescent units (RFU) measured from a vial containing both the PLpro peptide and DEVD peptide (internal processing control). **A)** Negative result: The relative fluorescence units (RFU) from PLpro cleavage activities (top) do not noticeably increase over 60 minutes whereas the RFU from cleavage of the internal processing control peptide do (bottom); the results indicate that the subject was not actively infected with SARS-CoV-2. **B)** Invalid result: RFU from both the PLpro and internal processing control peptides do not increase. The test is invalid. **C)** Positive result: The RFU from both PLpro and internal processing control peptides increases over 60 minutes. This result indicates that the subject was infected with SARS-CoV-2.

<https://doi.org/10.1371/journal.pone.0309305.g009>

In this study, the RFU from the Quanti Vial revealed that lysates from saliva contained approximately twice as much material based on nucleic acid content compared to lysate from tongue scrape (sum of all sample RFU = 4,347 versus 2,545 RFU, respectively). In 6 cases, tongue scrape samples and in 4 cases saliva samples did not contain sufficient material according to the internal processing control, DEVD, using as cutoff a ratio of <10 (Δ RFU PLpro/RFU QuantiVial)*100. The first 13 tongue scrape samples that were collected by the same operator included 5 with insufficient material whereas the last 11 samples included only 1 with insufficient material (S1 Table), indicating that operator training (more rigorous, yet still painless scraping) must be improved for the test to perform as a POCT and that, overall, saliva is a preferred specimen.

Comparison between the standard of care RT-PCR and protease test. In this first study, the negative percent agreement (NPA) and positive percent agreement (PPA) between the protease test and clinical LIAT RT-PCR were low: The PPA was 45.5% and 86% for saliva and tongue scrape, and the NPA 50% and 33%, respectively. This result was not unexpected given that different specimen types were used for RT-PCR (nasal mid-turbinate) and the protease test (saliva and tongue scrape) that may have had different viral loads [55]. Further, there were delays in collecting specimens for the protease test after RT-PCR results were returned: 6

samples were collected 0–10 hours after RT-PCR results were returned, 14 were collected between 10–24 hours later, and 3 were collected after more than 24 hours (S1 and S2 Tables). It is plausible that infections may have cleared in the RT-PCR positive cohort and were not detectable by the protease test, or infections had not yet been detected in the RT-PCR negative cohort but were detectable with the protease test. To better control for these variables—varying specimen types and collection times—a second clinical study was initiated using only saliva specimens that were split for testing with the SARS-CoV-2 protease assay and in-house RT-PCR.

SARS-CoV-2 PLpro and MPro activities relative to RT-PCR in saliva. In a second study, 22 patients with COVID-19 like symptoms were prescreened with LIAT RT-PCR performed on nasal mid turbinate specimens at the University of New Mexico Emergency Care Unit. Saliva (500 μ l) was collected on the same day the LIAT RT-PCR result was returned from 10 patients who tested positive and from 10 patients who tested negative. Two enrolled patients were not able to produce sufficient saliva and were excluded from the study. Each specimen was divided, and one half used for protease testing. RNA was extracted from the other half and analyzed using real time loop-mediated isothermal amplification (RT-LAMP) and endpoint RT-PCR with subsequent gel electrophoresis. Three patients with discordant results were sampled again 5 days later.

The protease tests were performed in 384-well plates and fluorescence was measured in a fluorescence plate reader. The delta RFU, and the ratios ($\text{delta RFU}_{\text{protease}} / \text{RFU}_{\text{Quanti dye}} \times 100$) were calculated using GraphPad Prism. The results are shown in Table 4. One sample did not contain sufficient material according to the LoD determined by Quanti dye (patient 19b, see Table 4) and one patient (# 13) had consumed a drink containing a blue dye 1 hour prior to providing their saliva sample that may have interfered with the fluorescence measurements. Results from these patients were excluded from further analysis.

The cutoff value of 27.7 for PLpro ratio was determined as described in methods. Test values equal or greater than this value were considered positive.

The LoD for specimen lysate was determined using Quanti dye as described in methods and was $\leq 196,858$ RFU and 169,888 RFU for MPro and PLpro, respectively (S1 Fig). Samples in which the RFU from Quanti dye was below this cutoff were evaluated as invalid.

Correlation between MPro and PLpro activities in saliva. In this study, the SARS-CoV-2 MPro activities were measured in addition to the PLpro activities, in order to increase the confidence in our data. The slope m (8.688 \pm 1.38) was calculated from the formula $y = mx + b$, with b is the Y intercept and m is the slope. The y intercept was 363000 \pm 215000. The correlation between the MPro and PLpro response was significant across 20 samples tested: the Pearson r value = 0.8224 [95% Confidence interval 0.6059 to 0.9255], $R^2 = 0.6764$, and P (one tailed) = < 0.0001 , indicating a high likelihood that the fluorescent signal increases were a result of peptide cleavage by SARS-CoV-2 proteases rather than peptide cleavage by other proteases that may be active in the lysates (Fig 10).

Correlation between LIAT RT-PCR, RT-LAMP, and endpoint RT-PCR on NMT and saliva samples. The initial RT-PCR results (not including results from serial testing) using LIAT, LAMP and endpoint RT-PCR agreed for all samples that tested positive with LIAT RT-PCR using a cutoff of < 30 minutes for LAMP and > 50 ratio SARS-CoV-2 amplicon/RNase P amplicon for endpoint RT-PCR (Table 4). However, in 8 cases that were negative with LIAT RT-PCR, late signals between 32–52 minutes were observed with RT-LAMP. Since with RT-LAMP it cannot be determined whether these late RT-PCR signals resulted from SARS-CoV-2 amplicons or from primer dimers with which the fluorescent dye intercalates, RNA samples were amplified using endpoint RT-PCR and the PCR products separated on an agarose gel. An example of 9 samples (patient IDs 1–11) is shown in Fig 11.

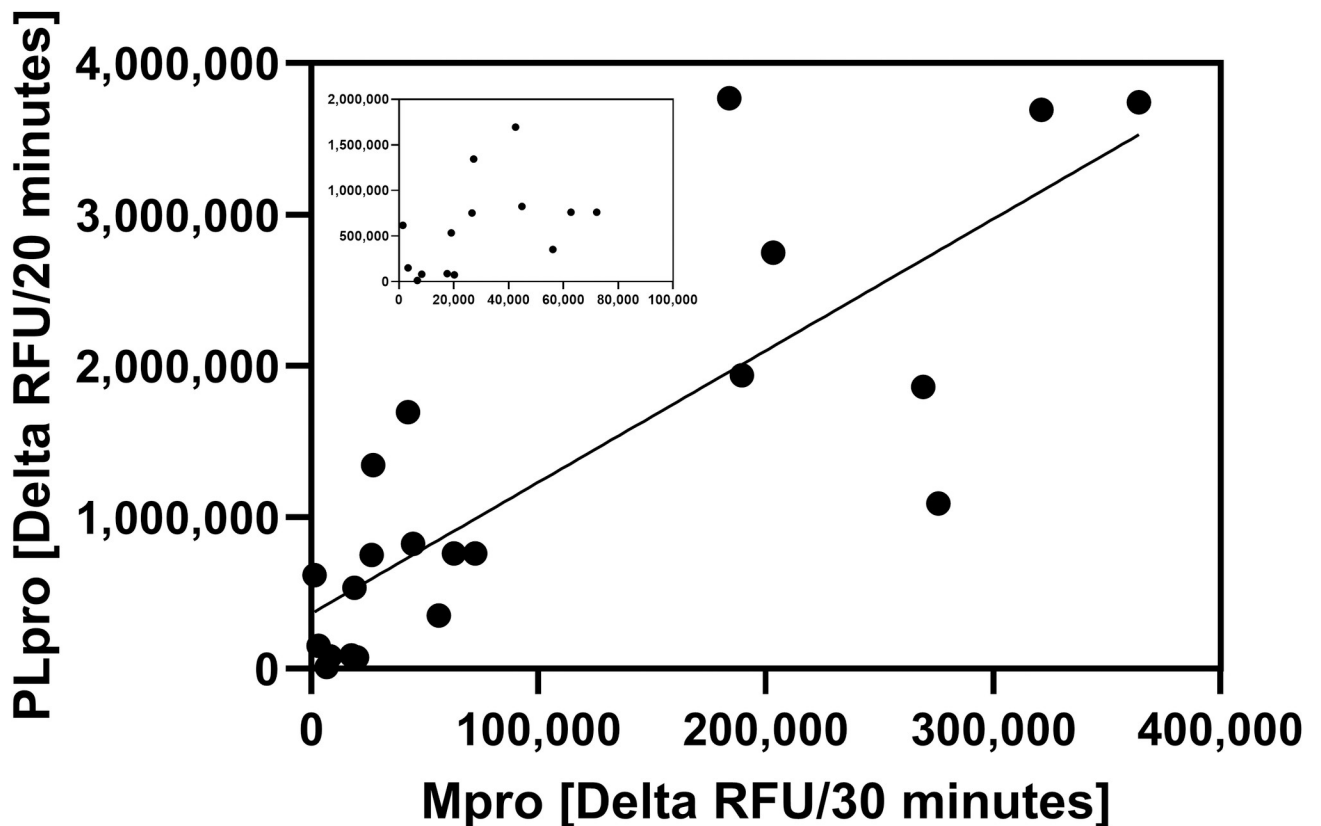


Fig 10. Correlation between SARS-CoV-2 MPro and PLpro activities. The Pearson r correlation between the delta RFU in x2 replicates from the Mpro and PLpro assays from 20 patient specimens was determined using GraphPad Prism. Data points with low RFU values are resolved in the inset.

<https://doi.org/10.1371/journal.pone.0309305.g010>

The results show strong amplification of the SARS-CoV-2 N1 gene in 3 samples that tested positive with LIAT and RT-LAMP (patient IDs 4, 8, and 9) and weak amplification in 4 samples that tested negative with LIAT RT-PCR and were late positive with RT-LAMP (patient

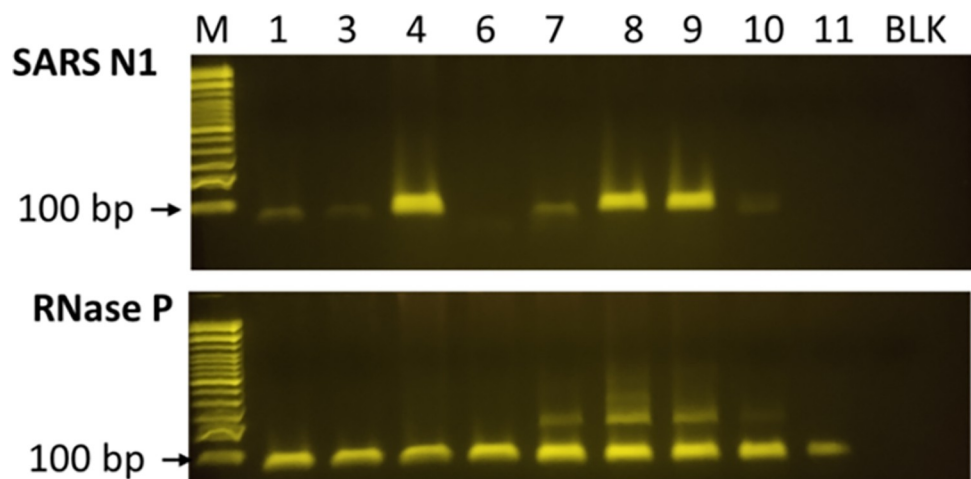


Fig 11. Agarose gel electrophoresis of RT-PCR amplicons. RNA was isolated from saliva specimens and reverse transcribed and amplified using endpoint RT-PCR mix containing SARS-CoV-2 N1 primers (top) or RNase P control primers (bottom) and separated on a 2% agarose gel. BLK = reaction without RNA. M = 100 base pair ladder, the 100 bp band is indicated by an arrow.

<https://doi.org/10.1371/journal.pone.0309305.g011>

Table 2. Summary of results obtained from parallel testing of saliva samples with the SARS-CoV-2 protease test and LIAT RT-PCR in patients suspected of COVID-19.

		LIAT RT-PCR		
		Positive	Negative	Total
PLpro Ratio delta RFU	Positive	7	6	13
	Negative	2	4	6
	Total	9	10	19
Positive Agreement		= 78% (7/9)		
Negative Agreement		= 40% (4/10)		

<https://doi.org/10.1371/journal.pone.0309305.t002>

IDs 1, 3, 7, and 10). 2 samples that were negative with LIAT and RT-LAMP did not contain amplicons (patient IDs 6 and 11). All samples were positive for the human RNaseP gene. To normalize for the amount of amplifiable RNA in the samples, the ratio was calculated between the integrated intensities of the SARS-CoV-2 amplicons and the RNase P gene (see Table 4).

PPA and NPA depends on the type of RT-PCR test used as comparator. The negative percent agreement (NPA) and positive percent agreement (PPA) of the SARS-CoV-2 test was calculated relative to LIAT RT-PCR using the normalized delta PLpro RFU (ratio RFU) from Table 4. Results from serial testing are not considered and one specimen from the RT-PCR positive cohort was evaluated as invalid with the protease test and is not included in the analysis shown in Table 2.

The sensitivity of detection was high, but the specificity was low due to 6 positives that were not detected using LIAT RT-PCR.

In contrast, when endpoint RT-PCR was used as a comparator, the PPA and PPA were 87.5% and 100% (Table 3). Two specimens that tested positive after 5 days (specimen ID 14b and 21b) are included in the RT-PCR positive cohort. Of the 2 false negatives detected, one is from a patient (patient 19) with a high Ct value of 35 in LIAT RT-PCR, suggesting that residual, non-infectious RNA may have been detected.

Earlier detection of infection with the SARS-CoV-2 protease test than with LIAT RT-PCR. One sample (14a) that tested negative with all three RT-PCR tests exhibited very strong delta RFU from the MPro and PLpro peptides (Table 4). The subject provided another sample 5 days later and the specimen (14b) was retested, and showed a positive result in endpoint RT-PCR. The normalized PLpro and MPro protease activities in sample 14b were approximately 2-fold higher than those obtained previously in sample 14a (3.4 and 12 for MPro and 63.4 and 122.4 for PLpro in samples 14a and 14b respectively). Endpoint RT-PCR was low positive in 14b (ratio N1/RNase P = 17). The results indicate that the SARS-CoV-2 protease test may have detected an infection before extracellular viral fragments were produced in quantities that could be measured by RT-PCR. Likewise, serial testing of patient 21,

Table 3. Summary of results obtained from parallel testing of saliva samples with the SARS-CoV-2 protease test and endpoint RT-PCR in patients suspected of COVID-19. The agreement was significant ($p = 0.0073$) using Chi square with Yates correction and 0.0103 using Fisher's exact test (2-tailed or 1-tailed).

		Endpoint RT-PCR		
		Positive	Negative	Total
PLpro Ratio delta RFU	Positive	14	0	14
	Negative	2	3	5
	Total	16	3	19
Positive Agreement		= 87.5% (14/16)		
Negative Agreement		= 100% (3/3)		

<https://doi.org/10.1371/journal.pone.0309305.t003>

Table 4. Results of saliva specimen testing. The results of testing with LIAT RT-PCR, RT-LAMP and endpoint RT-PCR (EP) are shown in comparison to the results of the Mesa Photonics MPro and PLpro tests. The delta RFU from 2–4 separate experiments with x2-4 replicates for Quanti Dye and PLpro were averaged (Δ mean) and the means normalized relative to the mean RFU from Quanti Dye. The cutoff value for specimen quantity was determined using Quanti Dye RFU of 169,888 RFU. Specimens with a value ≥ 27.7 for PLpro Ratio were considered positive.

Patient	RT-PCR			Quanti Dye		MPro				PLPro			
	LIAT	LAMP	EP	mean	CV	Δ mean	CV	Ratio	CV	Δ mean	CV	Ratio	CV
1	NDE	48	32	987,217	13.0	72,128	13.0	8.1	18.37	865,061	12.0	87.6	16.4
3	NDE	44	34	739,414	13.1	56,135	9.0	7.6	15.90	351,941	27.0	47.6	30.0
4	19	21	190	1,921,140	14.5	269,173	53.0	14.0	54.95	1,862,801	23.0	97.0	27.2
6	NDE	44	0	462,743	2.0	20,169	28.0	4.4	28.07	74,694	8.4	16.1	8.6
7	NDE	34	21	1,184,149	15.3	1,389	44.0	0.1	46.58	616,779	3.0	52.1	15.6
8	27	20	104	1,523,219	2.8	27,261	2.1	1.8	3.53	1,343,877	3.5	88.2	4.5
9	14	18	137	530,869	9.2	8,317	16.0	1.6	18.48	81,256	21.6	15.3	23.4
10	NDE	42	11	1,056,333	8.9	15,731	15.0	1.5	28.67	121,272	15.0	11.5	20.5
11	NDE	42	3	780,281	6.6	6,717	16.5	0.9	17.76	12,037	91.3	1.5	91.6
12	18	22	54	1,504,312	2.6	42,509	1.2	2.8	2.88	1,694,917	3.7	112.7	4.5
13*	13	16	209	817,452	9.4	6,990	31.0	0.9	32.38	130,816	12.0	16.0	15.2
14a	NDE	NDE	0	1,300,441	3.0	44,856	11.0	3.4	11.41	823,884	5.0	63.4	5.9
14b	ND	46	17	1,583,744	4.3	189,507	5.0	12.0	6.61	1,939,194	2.7	122.4	5.1
15	14	18	68	2,493,530	4.4	183,788	8.0	7.4	9.11	3,768,399	5.0	151.1	6.6
16	15	18	95	1,380,316	8.1	19,103	6.3	1.4	10.32	534,755	5.3	38.7	9.7
17	NDE	NDE	27	2,230,545	3.8	26,651	11.0	1.2	11.64	752,027	4.8	33.7	6.1
18	16	22	145	2,370,319	1.5	203,135	8.5	8.6	8.63	2,749,004	10.0	116.0	10.1
19	35	22	92	1,014,791	8.5	17,596	31.3	1.7	32.39	87,800	26.8	8.7	28.1
19b**	ND	26	82	137,574	10.6	4,262	9.0	3.1	13.90	-116,505	-33.3	-84.7	35.0
20	NDE	32	32	1,921,990	2.7	275,902	7.7	14.4	8.12	1,091,985	3.7	56.8	4.5
21a	NDE	50	11	2,059,971	2.2	321,324	7.0	15.6	7.33	3,692,954	1.7	179.3	2.7
21b	ND	52	20	2,296,219	2.1	364,133	3.5	15.9	4.07	3,740,001	6.0	162.9	6.3
22	26	22	83	2,066,863	2.0	62,769	5.7	3.0	6.00	761,528	2.3	36.8	3.1

*Fluorescence interference

**Not enough sample.

<https://doi.org/10.1371/journal.pone.0309305.t004>

who provided a second sample after 5 days showed a high level of SARS-CoV-2 protease activity on both days of testing, in absence of a positive LIAT RT-PCR result, but with late signals in RT-LAMP (50 and 52) and endpoint RT-PCR (ratio N1/RNAase P = 11 and 20) on days 1 and 5 of testing (Table 4).

The normalized ratios of PLpro activities from the initial day of testing can be divided into three groups: 8 samples with high PLpro activity (ratios between 85–179 RFU), 7 samples with moderate PLpro activity (ratios between 24–63 RFU) and 4 samples with low PLpro activities (ratios between 2–17 RFU), of which 3 samples tested negative with endpoint RT-PCR. The distribution is shown in a box and whisker plot (Fig 12). The two presumptive false negative PLpro specimens are included in the RT-PCR positive cohort.

Discussion

In this work, we have shown feasibility of a SARS-CoV-2 PLpro activity-based assay as a rapid and simple diagnostic test for detecting active infections in patient saliva, potentially earlier and more accurately than is possible with diagnostic RT-PCR. The test was performed in a POCT site by minimally trained operators or automated in a laboratory setting using a

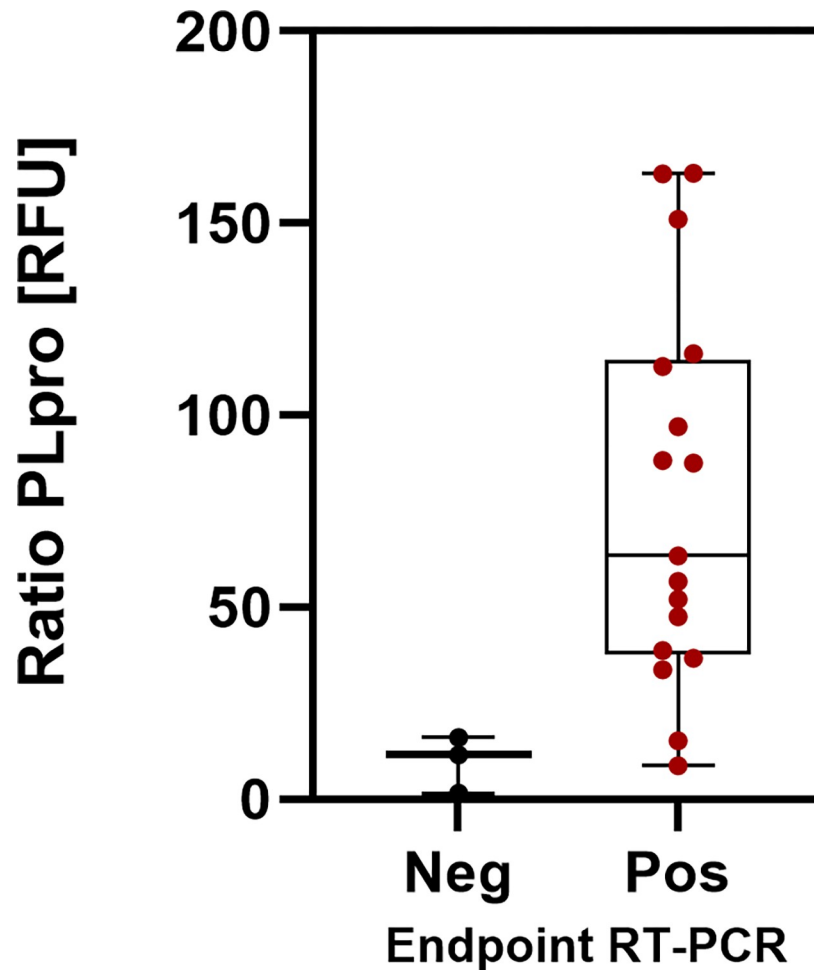


Fig 12. Box and whiskers plot of mean, max and min of PLpro ratios in a negative (Neg) and positive (Pos) cohort with endpoint RT-PCR as a comparator.

<https://doi.org/10.1371/journal.pone.0309305.g012>

fluorescence plate reader. The specificity of SARS-CoV-2 PLpro peptide cleavage was supported by data from VeroE6 cells infected with SARS-CoV-2. In addition, we demonstrate the application of the platform for screening of antiviral targeted drugs and neutralizing agents at lower time and cost and greater ease of use compared to current viral proliferation assays.

PLpro activity as a marker of SARS-CoV-2 infection

Activity-based diagnostics has been described for SARS-CoV-2 MPro [7, 9, 56]. In this study, we chose SARS-CoV-2 PLpro as the target, due to its role as a target for drugs that may reduce not only viral proliferation but also improve the host innate immune response. Detecting PLpro activity in crude, unprocessed cellular lysates was successful due to a rigorous design and optimization of the test platform to ensure that the reporter peptide was cleaved predominantly by SARS-CoV-2 PLpro and not significantly by papain-like proteases from other human coronaviruses or by other proteases that are present in crude lysates. The specificity of cleavage was accomplished by i) using fluorophores that fluoresce only when the bond between the terminal amino acid and the fluor is cleaved, whereas any potential cleavage by other proteases between upstream amino acids does not result in significant fluorescent

signals; ii) increasing the sensitivity of detection by designing 16-mer and 74-mer peptides composed of amino acids from the ISG15 protein that PLpro is known to preferentially bind and cleave [44]. In this study ISG15-based peptides resulted in a 43-fold increase in detection sensitivity in biochemical assays compared to the minimal tetrapeptide. In addition, the background cleavage of ISG15-based peptides was low, likely because only few deISGylating proteases are expressed in human cells that would cleave the ISG15-based peptides of the test, e.g., the ubiquitin-specific proteases USP5, USP16, and USP18 [57, 58]. Accordingly, we observed that cleavage of the PLpro ISG15-based peptide Pun74 by host cell proteases in lysates from uninfected VeroE6 cells was less than 10% relative to the cleavage in lysates from infected cells; iii) increasing the specificity of detection by incorporating unnatural amino acids into the LRGG cleavage site of the peptide. Specific cleavage of the ISG15-based peptides by recombinant PLpros from SARS-CoV and SARS-CoV-2 was observed, whereas no significant cleavage was observed by recombinant papain-like proteases from the other human coronaviruses (HCoV's MERS, OC43, NL62, 229E, and HKU1) or by the deISGylating human USP18 protease [48].

Comparison of saliva and tongue scrape specimens in a PoC test. The test was performed by minimally trained operators using a battery-operated fluorometer and without a need for precision volumetric control, thus making the test compatible with use in remote and hard to reach locations. Fluorescence increases were measured for 60 minutes, although 30 minutes was shown to be sufficient. In this POCT study, dual fluorescence from an internal processing control peptide (DEVD₂-R110) and the SARS-CoV-2 PLpro peptide (Pun16-AMC) was monitored in the same sample vial. Unfortunately, 26% (6 out of 23 samples) of the tongue scrape specimens did not contain sufficient amount of material according to the cutoff value set for the internal processing control DEVD. The high failure rate of tongue scrapes could be explained by an initial hesitancy of the operator to scrape vigorously as the majority of invalid samples were obtained during the first half of the study and the specimen quantity increased with operator experience. The protocol must be improved for the test to perform as a POCT. Saliva had a lower rate of invalid specimens (17%, 4 out of 23 samples), but some patients had difficulty producing the amounts of saliva required for the test (0.5 ml), especially older patients and those taking certain vitamin supplements and medication. In those cases, and for young children, tongue scrape specimens deserve future consideration.

Several limitations of this study must be noted. The experiments could be performed only once, the sample size was limited, and the pretest probability was high since only cases with strong clinical signs of COVID-19 were included. More than half of the specimens for the protease test were collected 10 to 48 hours after results from RT-PCR were returned, and unsurprisingly, the agreement with RT-PCR performed on nasopharyngeal swabs was low (PPA = 86% and 46%, NPA = 33% and 50% in tongue scrapes and saliva, respectively). It is plausible that infections in the RT-PCR positive cohort had cleared before specimens were collected for the protease test or had not yet been detected in the RT-PCR negative cohort in which 5 patients tested positive with the protease test. Further, different types of specimens were used—nasopharyngeal swabs (NPS) for RT-PCR and saliva for the protease test—that reportedly carry different viral loads [55].

SARS-CoV-2 RT-PCR in saliva

To minimize specimen collection failures and inconsistencies between RT-PCR and PLpro results due to different specimen types and collection times, we conducted a second pilot study, in which saliva specimens were collected on the same day that diagnostic RT-PCR results were returned. The saliva was split for SARS-CoV-2 protease testing and for in-house RT-PCR. We chose real time RT-LAMP since its performance in saliva was reported to equal

that of RT-PCR in a workplace surveillance study [59]. However, a drawback of real time RT-LAMP is that late signals resulting from true SARS-CoV-2 amplification products cannot be distinguished from primer dimers that readily form due to the large number of primers used in LAMP (6 per target) and their length (40–50 bases) [60]. To distinguish between those artefacts and SARS-CoV-2 amplicons, endpoint RT-PCR was performed using SARS-CoV-2 N1 and internal control RNase P primers with sequences corresponding to those recommended in 2020 by the CDC for SARS-CoV-2 testing. The products were separated by gel electrophoresis and the ratio of SARS-CoV-2 amplicons relative to control amplicons calculated. This may have been an imperfect analysis since the positive control primers originally recommended by the CDC are located in the same exon and it therefore cannot be distinguished whether the amplicons were derived from RNA or DNA, i.e., false negatives may have been obtained from samples in which RNA had degraded [45, 61]. Nevertheless, the agreement between the three RT-PCR test was 100% when a Ct value of ≤ 30 minutes was selected for RT-LAMP and a ratio N1/RNase P ≥ 50 for endpoint RT-PCR. However, in 8 cases, late signals ≥ 30 minutes were observed with RT-LAMP and ratios between N1/RNase P ≥ 20 for endpoint RT-PCR in 5 samples that were negative with LIAT RT-PCR.

The dramatic differences of positivity between LIAT RT-PCR (10 positives of 20) and endpoint RT-PCR (16 positives of 20) deserves further consideration. One explanation for the divergent results is that with LIAT RT-PCR samples with cycle threshold (Ct) values above 35 are reported as negative whereas we performed endpoint RT-PCR for 40 cycles, which may have increased the numbers of positives. Another factor is that endpoint RT-PCR was performed on RNA isolated from saliva, whereas LIAT was performed using nasal swabs. Reports show that there is a high degree of variability in detecting SARS-CoV-2 RNA among different specimen types that were collected at the same time from the same person [62]. One report showed a RT-PCR test positivity rate of 52.6% in nasopharyngeal swab specimens compared to 92.14% in saliva from the same patients, as well as higher viral loads and prolonged shedding in saliva [55].

Positive and negative agreement between SARS-CoV-2 ABDx assays and RT-PCR using saliva

When the results of this study were compared to those from endpoint RT-PCR, the sensitivity was 87.5% (14 of 16) and the specificity 100%, whereas the sensitivity was 78% and the specificity 40% when using diagnostic LIAT RT-PCR as a comparator (Tables 1 and 2). Several arguments can be made in support of the protease test results: 1) the normalized ratios >24 of MPro and PLpro activities corresponded with the results from endpoint RT-PCR (15 positives out of 19 specimens included in the study); 2) A significant correlation was measured between the SARS-CoV-2 PLpro and MPro proteases (Pearson $r = 0.8224$, Fig 10); 3) Although the study included only a small number of patients, the high number of positives detected is plausible because the study took place during the Omicron epidemic wave in New Mexico from the beginning of June to the end of September 2023 when test positivity trends peaked at 14.3% [63]. Further, the study included only patients with severe COVID-19 symptoms requiring emergency medicine services, thus increasing the pre-test probability of COVID-19.

Only 2 presumptive false negative results were observed in the protease test relative to endpoint RT-PCR: patient 9 with a PLpro ratio = 15.3 versus ratio endpoint RT-PCR = 137 and patient 19 with a PLpro ratio = 8.7 versus ratio endpoint RT-PCR = 92). This patient had a late CT value of 35 with diagnostic LIAT PCR and may no longer have been harboring an active infection, as indicated by the low SARS-CoV-2 PLpro activity.

A presumptive false positive result relative to endpoint RT-PCR was observed in patient 14 (normalized ratio PLpro = 63.4 versus endpoint RT-PCR ratio = 0; see [Table 4](#)) but serial testing after 5 days strongly indicated that the PLpro test had accurately detected the presence of an infection; the normalized PLpro ratio doubled from 63.4 to 122.4 and an amplicon was detected in endpoint RT-PCR in the second specimen collected (ratio N1/RNAseP = 17). A second presumptive false positive (patient ID 21) became positive in endpoint RT-PCR after 5 days.

Limitations

This study included only a limited number of clinical specimens with a high COVID-19 pre-test probability as a proof-of-concept for the performance of the SARS-CoV-2 activity assay. A substantially larger set of diverse clinical samples is needed to reliably estimate the sensitivity and specificity of the assay. Additionally, the small set of serial samples from patients with incongruent results is only an indication that the PLpro ABDx assay might detect SARS-CoV-2 infections earlier and within a narrower window than RT-PCR. If verified, earlier and more accurate detection would have tremendous implications for patient management and infection control.

SARS-CoV-2 PLpro activity platform for detection of any variant

It is expected that the PLpro activity assay will detect any SARS-CoV-2 variant. Although mutations in PLpro do occur, they do not affect the catalytically active regions which would produce a false negative protease test result because this would interfere with viral survival. Mutations are reported in other areas of PLpro that may affect substrate binding [35]. However, our reporter peptides are 17 and 74 amino acids in length and unlikely to lose their ability to bind to the enzyme substrate binding site in the event of single amino acid substitutions. Future testing of variants in cultured cells is planned to examine this.

Application of SARS-CoV-2 ABDx platform for antiviral screening

The data presented here also support the application of the protease platform as a screening tool for antiviral drugs. In our study, the inhibition value for the PLpro inhibitor GRL0617 in VeroE6 cells was 38.3 μ M ([Fig 6](#)), which is in close agreement to the effective inhibitory concentration of $21 \pm 2\mu$ M reported in a cell-based assay using cytopathic effect (CPE) as readout [50]. Currently, only 2 oral antiviral drugs are approved for use in the United States: Niraparvir (a component in Paxlovid) that targets MPro, and molnupiravir, a nucleoside analog developed by Merck targeting RNA-dependent RNA polymerase (RdRp) [64, 65]. Over the past 3 years variants with mutations in MPro have caused drug resistance under therapeutic pressure while concerns have been raised about molnupiravir's capacity to trigger SARS-CoV-2 mutations [66–68]. It is therefore important to study additional therapeutic targets, such as SARS-CoV-2 PLpro. Inhibiting the dual functions of PLpro—suppression of the innate immune response by cleaving ISG15 and processing of the viral polyprotein—have prompted drug development efforts, but to date, none of the promising drug candidates have advanced to animal models [15, 41, 69]. One explanation is that most biochemical studies examined only the minimal proteolytic domain of PLpro without considering the other domains in SARS-CoV-2 proteins that influence PLpro activity and function [41]. Although this limitation is overcome by tests that measure the extent of drug-induced cytopathic effect (CPE) in cells or quantify the amount of viral RNA in response to inhibition, these phenotypic assays take days to complete and require several user steps. Assays using genetically modified SARS-CoV-2 strains or replicons are faster and simpler but are suitable only for the virus strains they have

been established for [70]. A recent SARS-CoV-2 Flip-GFP-based reporter assay can be used in cells but monitors the activity of recombinant, unnatural PLpro, while an assay using a peptide construct for dual monitoring of MPro and PLpro activities in cells may suffer from inducing an unnatural PLpro conformation [16, 42]. In contrast, the SARS-CoV-2 PLpro assay described here is a simple add-and-measure homogeneous assay that measures the activity of natural, full length PLpro and can be scaled up to run in 96-well or 384 well plates. Time course data demonstrates that SARS-CoV-2 PLpro activity or inhibition can be detected in as little as 6 hours after infection with 0.1 MOI (Fig 5) or after a 24-hour incubation with an MOI of 0.01 with minimal user steps. Including caspase-induced cleavage of the DEVD peptide in the same well as PLpro peptide cleavage can normalize for the amount of cells/lysate present and provide additional information on cell health. In fact, one study relied solely on monitoring caspase activity to determine the activity of anti-SARS-CoV-2 antivirals and neutralization [70].

The assay platform also shows promise for detecting new neutralizing antibodies (Fig 7) that are urgently needed to combat the loss of efficacy of previously effective monoclonal therapeutics due to SARS-CoV-2 variants, as manifested by increased numbers of breakthrough infections in vaccinated individuals [71–75]. Our data demonstrates successful detection of neutralizing activity from patient serum and promises to be a rapid, low-cost alternative to other multi-step and laborious phenotypic assays, such as plaque reduction neutralization test (PRNT), fluorescent antibody virus neutralization (FAVN) assays, or immunological assays [43].

Conclusion

Functional activity-based diagnostic assays such as the SARS-CoV-2 PLpro assay presented here are gaining increasing importance as reliable tools for detecting pathogen infections. Significant advantages are that test reagents are inexpensive and can be synthesized in bulk for widespread distribution with minimal turnaround times. The cost efficiency and scalability of the test make it suitable to test asymptomatic and presymptomatic carriers in screening efforts. Further, our data indicates that the SARS-CoV-2 protease test may detect only active infections and possibly earlier than with RT-PCR. Early and accurate determination of whether a person is actively infectious is a critical factor in making treatment and quarantining decisions. The expected resistance of SARS-CoV-2 PLpro to mutations in emerging variants makes it a powerful surveillance tool to prepare for future outbreaks. Further, we demonstrate the potential of the assay platform for rapid and homogeneous cell-based screening of antiviral therapeutics against SARS-CoV-2.

This report encourages the application of the platform as an effective diagnostic for other infectious diseases, such as influenza, viral Hepatitis C, or mycobacterial tuberculosis, through careful selection of an appropriate enzyme and the design of a peptide that it specifically cleaves.

Supporting information

S1 File. Minimal data set.

(DOCX)

S1 Fig. Limit of Detection (LoD) for PLpro and MPro determined by Quanti Dye. Serial dilutions of lysates from patients who tested positive or negative for SARS-CoV-2 by RT-PCR were prepared in lysis buffer. Peptides cleaved by A) MPro or B) PLpro were reacted for 30 minutes with lysates. C) Quanti Dye was added to lysate in separate wells. Linear regression of the delta RFU was performed using GraphPad Prism and the 95% confidence bands of the best fit lines shown as dotted lines. The x intercepts of the reaction from positive (b2) and negative

(b1) lysates were calculated using the formula $x = (b_2 - b_1) / (m_1 - m_2)$, where b is the y intercept and m is the slope. The LoDs for the MPro and PLpro substrates were 6.4 μ l and 3.9 μ l lysate, respectively. Interpolation of these values to the linear fit from the Quanti Dye RFU was performed using the formula $y = mx + b$ and resulted in LoDs for Quanti Dye of 196,858 RFU for MPro and 169,888 RFU for PLpro peptides, respectively.

(TIF)

S2 Fig. DUB activities in lysates from cells infected with human coronaviruses. Top. Cells (~100,000) were infected (+) with 2 MOI (229E and OC43) or 1 MOI (NL63) and incubated for 24 hours. Control are uninfected cells (-). Lysates were prepared and incubated with ISG15-AMC or Ubiquitin-AMC and fluorescence monitored after 15 minutes. **Bottom.** Positive control peptides that are cleaved by ACE2 were added to separate wells containing lysates, demonstrating comparable quantities of active lysates from infected and uninfected cells. * the measurement was performed with higher instrument gain settings.

(TIF)

S3 Fig. Host cell lysis by Mesa Photonics lysis buffer. Representative microscopy images at 200X magnification for a cytotoxicity assessment of lysis buffer. Vero-E6 cells exposed to undiluted lysis buffer experienced significant cell death on the day of treatment. Dilutions of the lysis buffer at 1:10 or greater in viral growth media resulted in no observed cell death on both the day of treatment and 7 days post-treatment. Furthermore, when a detergent removal step was implemented, cells treated with undiluted lysis buffer exhibited no cytotoxic effects during the experiment period. Cells treated with water did not exhibit cytotoxicity, although limited small regions of the well displayed cell detachment which may be due to cell plating. However, cells began to regrow in these areas during 7 days of experiment, suggesting that the diluent used to prepare the lysis buffer did not cause cytotoxic effects.

(TIF)

S4 Fig. Host cell lysis by lysis buffer determined by cell viability staining. Cell viability fluorescence signals (Y-axis) were obtained from test and control groups. The x-axis denotes the dilution in viral growth media of lysis buffer, detergent-removed lysis buffer, and water (diluent control). The gray columns represent cells treated with lysis buffer without filtration through PDRSC; the blue columns correspond to cells treated with lysis buffer filtered through PDRSC; the red columns represent cells treated with water; and the green column represents 1X alamarBlue only group (background control). Two measurements were taken for each dilution in every sample group and 4 measurements for the 1X alamarBlue only control. Cells exposed to undiluted lysis buffer exhibited a 2-log reduction in absolute fluorescence signal compared to the other groups, and a similar fluorescence reading compared to 1X alamarBlue only background control group. This indicates complete host cell lysis which is consistent with the microscopic examination observations.

(TIF)

S5 Fig. Lysis buffer inactivation efficacy against SARS-CoV-2. Various dilutions of SARS-CoV-2 from two different lots were prepared from viral stock and combined with lysis buffer or VGM in a ratio of 1:9. Retained virus infectivity was determined by plaque assay. **A. Comparison of plaque formation in different treatment groups.** Healthy cell growth was observed in the no-virus control group (**panel 1**), whereas the group treated with undiluted lysis buffer (with or without virus) demonstrated significant cell death (**wells A1 in panel 2, 4-1 and 4-2**), whereas wells treated with diluted lysis buffer maintained a healthy cell monolayer (**wells A2-B3 in panel 2**). The virus-only control group (**panels 3-1 and 3-2**) formed plaques across all virus dilutions (from undiluted to 10,000-fold dilution). In contrast, the

group treated with virus in lysis buffer (wells A2-B2 in panels 4–1 and 4–2) showed no plaques, indicating effective inactivation of the virus by lysis buffer. The well with undiluted lysis buffer showed no crystal violet staining (**well A1 in panels 2, 4–1 and 4–2**) due to lysis buffer cytotoxicity. **B. Repeat of virus positive control in plaque formation assay:** To obtain better defined and countable plaques, we repeated the plaque assay using SARS-CoV-2 from the lots we tested in A with a higher concentration of CMC (3%) for sharper plaque formation. As shown in figure B, sharp and countable plaque are formed in infected VeroE6 cells treated with 1,000X-10,000X dilutions of virus. The titer of the virus lot V00193 was calculated as 4.2×10^6 pfu/mL and the titer of virus lot V00282 was calculated as 9.8×10^5 PFU/mL. The combined data suggest that lysis buffer is able to fully inactivate SARS-CoV-2, at least within these infectious titers, and that the virus inactivation effect is independent of the virus lot. (TIF)

S6 Fig. Comparison between the performance of Pun16-R110 and Pun74-R110 in lysates from saliva specimens. Lysates from specimens that demonstrated high (blue), moderate (purple), and low (pink) PLpro activity were reacted with A) Pun17-R110 and B) Pun74-R110 in wells of a 384 well plate. The delta RFU between the immediate read and the read after 30 minutes of reaction were calculated and graphed using GraphPad Prism. (TIF)

S1 Table. Results from PoC testing for SARS-CoV-2 infection in lysates from tongue scrape specimens from 23 patients. The cycle threshold (Ct) values obtained for 23 patients and the delay (hours) between return of diagnostic RT-PCR and sample collection are given. **Top.** PLpro. Relative fluorescence units (RFU) between the 60 minute and 0-minute reads PLpro activity and the delta RFU (Δ) are shown. The ratio between delta RFU and Quanti Vial (QV) was calculated and the mean determined. Invalid samples (INV), true positives (TP), false negatives (FN), true negatives (TN), and false positives (FP) are indicated. **Bottom.** DEVD. The ratio of delta RFU was calculated and the LoD detection determined as <10 ratio mean. (TIF)

S2 Table. Results from PoC testing for SARS-CoV-2 infection in lysates from saliva specimens from 23 patients. The cycle threshold (Ct) values obtained for 23 patients and the delay (hours) between return of diagnostic RT-PCR and sample collection are given. **Top.** PLpro. Relative fluorescence units (RFU) between the 60 minute and 0-minute reads of PLpro activity and the delta RFU (Δ) are shown. The ratio between delta RFU and Quanti Vial (QV) was calculated and the mean determined. Invalid samples (INV), true positives (TP), false negatives (FN), true negatives (TN) and false positives (FP) are indicated. **Bottom.** DEVD. The ratio of delta RFU was calculated and the LoD detection determined as <10 ratio mean. (TIF)

Acknowledgments

We thank Sarah Lavelle, Munia Omer and Kate Browning (University of New Mexico) for support with IRB submission and active recruitment.

Author Contributions

Conceptualization: Nileena Velappan, Steven Bradfute, Frauke H. Rininsland.

Formal analysis: William J. Bruno, Frauke H. Rininsland.

Funding acquisition: Frauke H. Rininsland.

Investigation: Chunyan Ye, Justin T. Baca, Frauke H. Rininsland.

Methodology: Anahi G. Jimenez-Campos, Lucas I. Maestas, Nileena Velappan, Chunyan Ye, Keith Wernsing, Yaniksa Mata-Solis, Steven Bradfute, Justin T. Baca, Frauke H. Rininsland.

Project administration: Silas C. Bussmann, Justin T. Baca, Frauke H. Rininsland.

Resources: Frauke H. Rininsland.

Supervision: Brian Beck, Justin T. Baca, Frauke H. Rininsland.

Validation: Frauke H. Rininsland.

Writing – original draft: William J. Bruno, Frauke H. Rininsland.

Writing – review & editing: Anahi G. Jimenez-Campos, William J. Bruno, Frauke H. Rininsland.

References

1. COVID-19—FIND. [cited 29 Jan 2024]. Available: <https://www.finddx.org/covid-19/>
2. Shi L, Wang L, Ma X, Fang X, Xiang L, Yi Y, et al. Aptamer-Functionalized Nanochannels for One-Step Detection of SARS-CoV-2 in Samples from COVID-19 Patients. *Anal Chem.* 2021; 93: 16646–16654. <https://doi.org/10.1021/acs.analchem.1c04156> PMID: 34847324
3. Peng Y, Pan Y, Sun Z, Li J, Yi Y, Yang J, et al. An electrochemical biosensor for sensitive analysis of the SARS-CoV-2 RNA. *Biosens Bioelectron.* 2021; 186: 113309. <https://doi.org/10.1016/j.bios.2021.113309> PMID: 33984795
4. Wang M, Lin Y, Lu J, Sun Z, Deng Y, Wang L, et al. Visual naked-eye detection of SARS-CoV-2 RNA based on covalent organic framework capsules. *Chem Eng J.* 2022; 429: 132332. <https://doi.org/10.1016/j.cej.2021.132332> PMID: 34539223
5. Myers R, Ruskiewicz DM, Meister A, Bartolomeu C, Atkar-Khattra S, Thomas CLP, et al. Breath testing for SARS-CoV-2 infection. *eBioMedicine.* 2023; 92: 104584. <https://doi.org/10.1016/j.ebiom.2023.104584> PMID: 37121096
6. Sharma R, Zang W, Tabartehfarahani A, Lam A, Huang X, Sivakumar AD, et al. Portable Breath-Based Volatile Organic Compound Monitoring for the Detection of COVID-19 During the Circulation of the SARS-CoV-2 Delta Variant and the Transition to the SARS-CoV-2 Omicron Variant. *JAMA Netw Open.* 2023; 6: e230982. <https://doi.org/10.1001/jamanetworkopen.2023.0982> PMID: 36853606
7. Yamauchi Y, Konno S, Omura N, Yoshioka N, Hingst A, Gütschow M, et al. Detection of Active SARS-CoV-2 3CL Protease in Infected Cells Using Activity-Based Probes with a 2,6-Dichlorobenzoyloxy-methyl Ketone Reactive Warhead. *ACS Chem Biol.* 2024; 19: 1028–1034. <https://doi.org/10.1021/acscchembio.4c00024> PMID: 38668705
8. Liang Q, Huang Y, Wang M, Kuang D, Yang J, Yi Y, et al. An electrochemical biosensor for SARS-CoV-2 detection via its papain-like cysteine protease and the protease inhibitor screening. *Chem Eng J.* 2023; 452: 139646. <https://doi.org/10.1016/j.cej.2022.139646> PMID: 36249721
9. Rut W, Groborz K, Zhang L, Sun X, Zmudzinski M, Pawlik B, et al. SARS-CoV-2 Mpro inhibitors and activity-based probes for patient-sample imaging. *Nat Chem Biol.* 2021; 17: 222–228. <https://doi.org/10.1038/s41589-020-00689-z> PMID: 33093684
10. Fan K, Wei P, Feng Q, Chen S, Huang C, Ma L, et al. Biosynthesis, Purification, and Substrate Specificity of Severe Acute Respiratory Syndrome Coronavirus 3C-like Proteinase. *J Biol Chem.* 2004; 279: 1637–1642. <https://doi.org/10.1074/jbc.M310875200> PMID: 14561748
11. Han Y-S, Chang G-G, Joo C-G, Lee H-J, Yeh S-H, Hsu JT-A, et al. Papain-Like Protease 2 (PLP2) from Severe Acute Respiratory Syndrome Coronavirus (SARS-CoV): Expression, Purification, Characterization, and Inhibition. *Biochemistry.* 2005; 44: 10349–10359. <https://doi.org/10.1021/bi0504761> PMID: 16042412
12. Goralbanya AE, Enjuanes L, Ziebuhr J, Snijder EJ. Nidovirales: Evolving the largest RNA virus genome. *Virus Res.* 2006; 117: 17–37. <https://doi.org/10.1016/j.virusres.2006.01.017> PMID: 16503362
13. Barretto N, Jukneliene D, Ratia K, Chen Z, Mesecar AD, Baker SC. The Papain-Like Protease of Severe Acute Respiratory Syndrome Coronavirus Has Deubiquitinating Activity. *J Virol.* 2005; 79: 15189–15198. <https://doi.org/10.1128/JVI.79.24.15189-15198.2005> PMID: 16306590

14. Klemm T, Ebert G, Calleja DJ, Allison CC, Richardson LW, Bernardini JP, et al. Mechanism and inhibition of the papain-like protease, PLpro, of SARS-CoV-2. *EMBO J*. 2020; 39. <https://doi.org/10.15252/embj.2020106275> PMID: 32845033
15. Jiang H, Yang P, Zhang J. Potential Inhibitors Targeting Papain-Like Protease of SARS-CoV-2: Two Birds With One Stone. *Front Chem*. 2022; 10: 822785. <https://doi.org/10.3389/fchem.2022.822785> PMID: 35281561
16. Cheng Y, Borum RM, Clark AE, Jin Z, Moore C, Fajtová P, et al. A Dual-Color Fluorescent Probe Allows Simultaneous Imaging of Main and Papain-like Proteases of SARS-CoV-2-Infected Cells for Accurate Detection and Rapid Inhibitor Screening. *Angew Chem Int Ed*. 2022; 61: e202113617. <https://doi.org/10.1002/anie.202113617> PMID: 34889013
17. Soleimany AP, Bhatia SN. Activity-Based Diagnostics: An Emerging Paradigm for Disease Detection and Monitoring. *Trends Mol Med*. 2020; 26: 450–468. <https://doi.org/10.1016/j.molmed.2020.01.013> PMID: 32359477
18. Babin BM, Fernandez-Cuervo G, Sheng J, Green O, Ordonez AA, Turner ML, et al. Chemiluminescent Protease Probe for Rapid, Sensitive, and Inexpensive Detection of Live *Mycobacterium tuberculosis*. *ACS Cent Sci*. 2021; 7: 803–814. <https://doi.org/10.1021/acscentsci.0c01345> PMID: 34079897
19. Muir RK, Guerra M, Bogoyo MM. Activity-Based Diagnostics: Recent Advances in the Development of Probes for Use with Diverse Detection Modalities. *ACS Chem Biol*. 2022; 17: 281–291. <https://doi.org/10.1021/acscchembio.1c00753> PMID: 35026106
20. Greenbaum D, Medzihradzsky KF, Burlingame A, Bogoyo M. Epoxide electrophiles as activity-dependent cysteine protease profiling and discovery tools. *Chem Biol*. 2000; 7: 569–581. [https://doi.org/10.1016/s1074-5521\(00\)00014-4](https://doi.org/10.1016/s1074-5521(00)00014-4) PMID: 11048948
21. Su Y, Ge J, Zhu B, Zheng Y-G, Zhu Q, Yao SQ. Target identification of biologically active small molecules via in situ methods. *Curr Opin Chem Biol*. 2013; 17: 768–775. <https://doi.org/10.1016/j.cbpa.2013.06.005> PMID: 23796909
22. Owusu D, Pomeroy MA, Lewis NM, Wadhwa A, Yousof AR, Whitaker B, et al. Persistent SARS-CoV-2 RNA Shedding Without Evidence of Infectiousness: A Cohort Study of Individuals With COVID-19. *J Infect Dis*. 2021; 224: 1362–1371. <https://doi.org/10.1093/infdis/jiab107> PMID: 33649773
23. Cevik M, Tate M, Lloyd O, Maraolo AE, Schafers J, Ho A. SARS-CoV-2, SARS-CoV, and MERS-CoV viral load dynamics, duration of viral shedding, and infectiousness: a systematic review and meta-analysis. *Lancet Microbe*. 2021; 2: e13–e22. [https://doi.org/10.1016/S2666-5247\(20\)30172-5](https://doi.org/10.1016/S2666-5247(20)30172-5) PMID: 33521734
24. Case JB, Bailey AL, Kim AS, Chen RE, Diamond MS. Growth, detection, quantification, and inactivation of SARS-CoV-2. *Virology*. 2020; 548: 39–48. <https://doi.org/10.1016/j.virol.2020.05.015> PMID: 32838945
25. Jeong HW, Kim S-M, Kim H-S, Kim Y-I, Kim JH, Cho JY, et al. Viable SARS-CoV-2 in various specimens from COVID-19 patients. *Clin Microbiol Infect*. 2020; 26: 1520–1524. <https://doi.org/10.1016/j.cmi.2020.07.020> PMID: 32711057
26. Ford L, Lee C, Pray IW, Cole D, Bigouette JP, Abedi GR, et al. Epidemiologic Characteristics Associated With Severe Acute Respiratory Syndrome Coronavirus 2 (SARS-CoV-2) Antigen-Based Test Results, Real-Time Reverse Transcription Polymerase Chain Reaction (rRT-PCR) Cycle Threshold Values, Subgenomic RNA, and Viral Culture Results From University Testing. *Clin Infect Dis*. 2021; 73: e1348–e1355. <https://doi.org/10.1093/cid/ciab303> PMID: 33846714
27. Binnicker MJ. Can Testing Predict SARS-CoV-2 Infectivity? The Potential for Certain Methods To Be Surrogates for Replication-Competent Virus. Humphries RM, editor. *J Clin Microbiol*. 2021; 59: e00469–21. <https://doi.org/10.1128/JCM.00469-21> PMID: 34346713
28. Arons MM, Hatfield KM, Reddy SC, Kimball A, James A, Jacobs JR, et al. Presymptomatic SARS-CoV-2 Infections and Transmission in a Skilled Nursing Facility. *N Engl J Med*. 2020; 382: 2081–2090. <https://doi.org/10.1056/NEJMoa2008457> PMID: 32329971
29. Singanayagam A, Patel M, Charlett A, Lopez Bernal J, Saliba V, Ellis J, et al. Duration of infectiousness and correlation with RT-PCR cycle threshold values in cases of COVID-19, England, January to May 2020. *Eurosurveillance*. 2020; 25. <https://doi.org/10.2807/1560-7917.ES.2020.25.32.2001483> PMID: 32794447
30. Platten M, Hoffmann D, Grosser R, Wisplinghoff F, Wisplinghoff H, Wiesmüller G, et al. SARS-CoV-2, CT-Values, and Infectivity—Conclusions to Be Drawn from Side Observations. *Viruses*. 2021; 13: 1459. <https://doi.org/10.3390/v13081459> PMID: 34452325
31. Bar-On YM, Flamholz A, Phillips R, Milo R. SARS-CoV-2 (COVID-19) by the numbers. *eLife*. 2020; 9: e57309. <https://doi.org/10.7554/eLife.57309> PMID: 32228860

32. Pinto AL, Rai RK, Brown JC, Griffin P, Edgar JR, Shah A, et al. Ultrastructural insight into SARS-CoV-2 entry and budding in human airway epithelium. *Nat Commun.* 2022; 13: 1609. <https://doi.org/10.1038/s41467-022-29255-y> PMID: 35338134
33. Puhach O, Meyer B, Eckerle I. SARS-CoV-2 viral load and shedding kinetics. *Nat Rev Microbiol.* 2022 [cited 22 Feb 2024]. <https://doi.org/10.1038/s41579-022-00822-w> PMID: 36460930
34. Høeg TB, Prasad V. Rapid antigen testing for COVID-19: Decreasing diagnostic reliability, potential detrimental effects and a lack of evidence to support continued public funding of community-based testing. *Public Health Pract.* 2023; 6: 100451. <https://doi.org/10.1016/j.puhip.2023.100451> PMID: 38075468
35. Perlinska AP, Stasiulewicz A, Nguyen ML, Swiderska K, Zmudzinski M, Maksymiuk AW, et al. Amino acid variants of SARS-CoV-2 papain-like protease have impact on drug binding. MacKerell A, editor. *PLOS Comput Biol.* 2022; 18: e1010667. <https://doi.org/10.1371/journal.pcbi.1010667> PMID: 36409737
36. Osório NS, Correia-Neves M. Implication of SARS-CoV-2 evolution in the sensitivity of RT-qPCR diagnostic assays. *Lancet Infect Dis.* 2021; 21: 166–167. [https://doi.org/10.1016/S1473-3099\(20\)30435-7](https://doi.org/10.1016/S1473-3099(20)30435-7) PMID: 32473662
37. Yi H. 2019 Novel Coronavirus Is Undergoing Active Recombination. *Clin Infect Dis.* 2020; 71: 884–887. <https://doi.org/10.1093/cid/ciaa219> PMID: 32130405
38. Shen Z, Xiao Y, Kang L, Ma W, Shi L, Zhang L, et al. Genomic Diversity of Severe Acute Respiratory Syndrome–Coronavirus 2 in Patients With Coronavirus Disease 2019. *Clin Infect Dis.* 2020; ciaa203. <https://doi.org/10.1093/cid/ciaa203> PMID: 32129843
39. Joyce RP, Hu VW, Wang J. The history, mechanism, and perspectives of nirmatrelvir (PF-07321332): an orally bioavailable main protease inhibitor used in combination with ritonavir to reduce COVID-19-related hospitalizations. *Med Chem Res.* 2022; 31: 1637–1646. <https://doi.org/10.1007/s00044-022-02951-6> PMID: 36060104
40. Paxlovid: A promising drug for the challenging treatment of SARS-COV-2 in the pandemic era—PubMed. [cited 15 Jan 2024]. Available: <https://pubmed.ncbi.nlm.nih.gov/36722557/>
41. Armstrong LA, Lange SM, Dee Cesare V, Matthews SP, Nirujogi RS, Cole I, et al. Biochemical characterization of protease activity of Nsp3 from SARS-CoV-2 and its inhibition by nanobodies. Ganesan A, editor. *PLOS ONE.* 2021; 16: e0253364. <https://doi.org/10.1371/journal.pone.0253364> PMID: 34270554
42. Ma C, Sacco MD, Xia Z, Lambrinidis G, Townsend JA, Hu Y, et al. Discovery of SARS-CoV-2 Papain-like Protease Inhibitors through a Combination of High-Throughput Screening and a FlipGFP-Based Reporter Assay. *ACS Cent Sci.* 2021; 7: 1245–1260. <https://doi.org/10.1021/acscentsci.1c00519> PMID: 34341772
43. Frische A, Brooks PT, Gybel-Brask M, Sækmose SG, Jensen BA, Mikkelsen S, et al. Optimization and evaluation of a live virus SARS-CoV-2 neutralization assay. Ito E, editor. *PLOS ONE.* 2022; 17: e0272298. <https://doi.org/10.1371/journal.pone.0272298> PMID: 35901110
44. Freitas BT, Durie IA, Murray J, Longo JE, Miller HC, Crich D, et al. Characterization and Noncovalent Inhibition of the Deubiquitinase and delSGylase Activity of SARS-CoV-2 Papain-Like Protease. *ACS Infect Dis.* 2020; 6: 2099–2109. <https://doi.org/10.1021/acsinfectdis.0c00168> PMID: 32428392
45. Real-time RT-PCR Primers and Probes for COVID-19 | CDC. [cited 27 Jun 2020]. Available: <https://www.cdc.gov/coronavirus/2019-ncov/lab/rt-pcr-panel-primer-probes.html>
46. Schneider CA, Rasband WS, Eliceiri KW. NIH Image to ImageJ: 25 years of image analysis. *Nat Methods.* 2012; 9: 671–675. <https://doi.org/10.1038/nmeth.2089> PMID: 22930834
47. The substrate selectivity of papain-like proteases from human-infecting coronaviruses correlates with innate immune suppression—PubMed. [cited 22 Mar 2024]. Available: <https://pubmed.ncbi.nlm.nih.gov/37130166/>
48. Rut W, Lv Z, Zmudzinski M, Patchett S, Nayak D, Snipas SJ, et al. Activity profiling and structures of inhibitor-bound SARS-CoV-2-PLpro protease provides a framework for anti-COVID-19 drug design. *Biochemistry.* 2020 Apr. <https://doi.org/10.1101/2020.04.29.068890> PMID: 32511411
49. Hug H, Los M, Hirt W, Debatin K-M. Rhodamine 110-Linked Amino Acids and Peptides as Substrates To Measure Caspase Activity upon Apoptosis Induction in Intact Cells. *Biochemistry.* 1999; 38: 13906–13911. <https://doi.org/10.1021/bi9913395> PMID: 10529236
50. Fu Z, Huang B, Tang J, Liu S, Liu M, Ye Y, et al. The complex structure of GRL0617 and SARS-CoV-2 PLpro reveals a hot spot for antiviral drug discovery. *Nat Commun.* 2021; 12: 488. <https://doi.org/10.1038/s41467-020-20718-8> PMID: 33473130
51. Xu H, Zhong L, Deng J, Peng J, Dan H, Zeng X, et al. High expression of ACE2 receptor of 2019-nCoV on the epithelial cells of oral mucosa. *Int J Oral Sci.* 2020; 12: 8. <https://doi.org/10.1038/s41368-020-0074-x> PMID: 32094336

52. NIH COVID-19 Autopsy Consortium, HCA Oral and Craniofacial Biological Network, Huang N, Pérez P, Kato T, Mikami Y, et al. SARS-CoV-2 infection of the oral cavity and saliva. *Nat Med.* 2021 [cited 7 Apr 2021]. <https://doi.org/10.1038/s41591-021-01296-8> PMID: 33767405
53. Li W, Moore MJ, Vasilieva N, Sui J, Wong SK, Berne MA, et al. Angiotensin-converting enzyme 2 is a functional receptor for the SARS coronavirus. *Nature.* 2003; 426: 450–454. <https://doi.org/10.1038/nature02145> PMID: 14647384
54. Tai W, He L, Zhang X, Pu J, Voronin D, Jiang S, et al. Characterization of the receptor-binding domain (RBD) of 2019 novel coronavirus: implication for development of RBD protein as a viral attachment inhibitor and vaccine. *Cell Mol Immunol.* 2020; 17: 613–620. <https://doi.org/10.1038/s41423-020-0400-4> PMID: 32203189
55. Beyene GT, Alemu F, Kebede ES, Alemayehu DH, Seyoum T, Tefera DA, et al. Saliva is superior over nasopharyngeal swab for detecting SARS-CoV2 in COVID-19 patients. *Sci Rep.* 2021; 11: 22640. <https://doi.org/10.1038/s41598-021-02097-2> PMID: 34811429
56. Todos Medical Announces Positive Initial Clinical Proof-of-Concept Data for a Rapid SARS-CoV-2 3CL Protease Detection Assay | BioSpace. [cited 23 Feb 2024]. Available: <https://www.biospace.com/article/releases/todos-medical-announces-positive-initial-clinical-proof-of-concept-data-for-a-rapid-sars-cov-2-3cl-protease-detection-assay/>
57. USP16 is an ISG15 cross-reactive deubiquitinase that targets pro-ISG15 and ISGylated proteins involved in metabolism—PubMed. [cited 23 Feb 2024]. Available: <https://pubmed.ncbi.nlm.nih.gov/38055744/>
58. Perng Y-C, Lenschow DJ. ISG15 in antiviral immunity and beyond. *Nat Rev Microbiol.* 2018; 16: 423–439. <https://doi.org/10.1038/s41579-018-0020-5> PMID: 29769653
59. Li Z, Bruce JL, Cohen B, Cunningham CV, Jack WE, Kunin K, et al. Development and implementation of a simple and rapid extraction-free saliva SARS-CoV-2 RT-LAMP workflow for workplace surveillance. Kalendar R, editor. *PLOS ONE.* 2022; 17: e0268692. <https://doi.org/10.1371/journal.pone.0268692> PMID: 35617204
60. Meagher RJ, Priye A, Light YK, Huang C, Wang E. Impact of primer dimers and self-amplifying hairpins on reverse transcription loop-mediated isothermal amplification detection of viral RNA. *The Analyst.* 2018; 143: 1924–1933. <https://doi.org/10.1039/c7an01897e> PMID: 29620773
61. Lee JS, Goldstein JM, Moon JL, Herzegh O, Bagarozzi DA, Oberste MS, et al. Analysis of the initial lot of the CDC 2019-Novel Coronavirus (2019-nCoV) real-time RT-PCR diagnostic panel. Kalendar R, editor. *PLOS ONE.* 2021; 16: e0260487. <https://doi.org/10.1371/journal.pone.0260487> PMID: 34910739
62. Chen L, Zhao J, Peng J, Li X, Deng X, Geng Z, et al. Detection of SARS-CoV-2 in saliva and characterization of oral symptoms in COVID-19 patients. *Cell Prolif.* 2020; 53: e12923. <https://doi.org/10.1111/cpr.12923> PMID: 33073910
63. Track Covid-19 in New Mexico: Latest Data and Maps—The New York Times. [cited 1 Mar 2024]. Available: <https://www.nytimes.com/interactive/2023/us/new-mexico-covid-cases.html>
64. Parums DV. Editorial: Current Status of Oral Antiviral Drug Treatments for SARS-CoV-2 Infection in Non-Hospitalized Patients. *Med Sci Monit.* 2022;28. <https://doi.org/10.12659/MSM.935952> PMID: 34972812
65. Kozlov M. Merck's COVID pill loses its lustre: what that means for the pandemic. *Nature.* 2021; d41586-021-03667-0. <https://doi.org/10.1038/d41586-021-03667-0> PMID: 34903873
66. Padhi AK, Tripathi T. Hotspot residues and resistance mutations in the nirmatrelvir-binding site of SARS-CoV-2 main protease: Design, identification, and correlation with globally circulating viral genomes. *Biochem Biophys Res Commun.* 2022; 629: 54–60. <https://doi.org/10.1016/j.bbrc.2022.09.010> PMID: 36113178
67. Iketani S, Mohri H, Culbertson B, Hong SJ, Duan Y, Luck MI, et al. Multiple pathways for SARS-CoV-2 resistance to nirmatrelvir. *Nature.* 2023; 613: 558–564. <https://doi.org/10.1038/s41586-022-05514-2> PMID: 36351451
68. Sanderson T, Hisner R, Donovan-Banfield I, Hartman H, Løchen A, Peacock TP, et al. A molnupiravir-associated mutational signature in global SARS-CoV-2 genomes. *Nature.* 2023; 623: 594–600. <https://doi.org/10.1038/s41586-023-06649-6> PMID: 37748513
69. Tan H, Hu Y, Jadhav P, Tan B, Wang J. Progress and Challenges in Targeting the SARS-CoV-2 Papain-like Protease. *J Med Chem.* 2022; 65: 7561–7580. <https://doi.org/10.1021/acs.jmedchem.2c00303> PMID: 35620927
70. Bojkova D, Reus P, Panosch L, Bechtel M, Rothenburger T, Kandler JD, et al. Identification of novel antiviral drug candidates using an optimized SARS-CoV-2 phenotypic screening platform. *iScience.* 2023; 26: 105944. <https://doi.org/10.1016/j.isci.2023.105944> PMID: 36644320

71. Iketani S, Liu L, Guo Y, Liu L, Chan JF-W, Huang Y, et al. Antibody evasion properties of SARS-CoV-2 Omicron sublineages. *Nature*. 2022; 604: 553–556. <https://doi.org/10.1038/s41586-022-04594-4> PMID: 35240676
72. Liu L, Iketani S, Guo Y, Chan JF-W, Wang M, Liu L, et al. Striking antibody evasion manifested by the Omicron variant of SARS-CoV-2. *Nature*. 2022; 602: 676–681. <https://doi.org/10.1038/s41586-021-04388-0> PMID: 35016198
73. Gruell H, Vanshylla K, Korenkov M, Tober-Lau P, Zehner M, Münn F, et al. SARS-CoV-2 Omicron sublineages exhibit distinct antibody escape patterns. *Cell Host Microbe*. 2022; 30: 1231–1241.e6. <https://doi.org/10.1016/j.chom.2022.07.002> PMID: 35921836
74. Lin D-Y, Xu Y, Gu Y, Zeng D, Wheeler B, Young H, et al. Effects of COVID-19 vaccination and previous SARS-CoV-2 infection on omicron infection and severe outcomes in children under 12 years of age in the USA: an observational cohort study. *Lancet Infect Dis*. 2023; 23: 1257–1265. [https://doi.org/10.1016/S1473-3099\(23\)00272-4](https://doi.org/10.1016/S1473-3099(23)00272-4) PMID: 37336222
75. Zhou H, Dcosta BM, Landau NR, Tada T. Resistance of SARS-CoV-2 Omicron BA.1 and BA.2 Variants to Vaccine-Elicited Sera and Therapeutic Monoclonal Antibodies. *Viruses*. 2022; 14: 1334. <https://doi.org/10.3390/v14061334> PMID: 35746806